University of Stavanger

Faculty of Science and Technology

MASTER'S THESIS

Study program/ Specialization: Master's in Biological Chemistry	Spring semester, 2014 Open / Restricted access
Writer: Tatiana Popovitchenko	…… (Writer's signature)
Faculty supervisor: Maria Doitsidou, Ph.D. External supervisor(s):	
Thesis title: **Mechanisms of TRP-channel mediated dopaminergic degeneration in C. elegans**	
Credits (ECTS): 60	
Key words: Neurodegeneration, dopaminergic degeneration, Parkinson's Disease (PD), lysosome, cell death, autophagy, necrosis	Pages: ……73…… + enclosure: ……79…. Stavanger, 16 June/2014

Front page for master thesis

Faculty of Science and Technology

Decision made by the Dean October 30th 2009

Abstract

One of the most common manifestations of dopaminergic degeneration in humans is in Parkinson's Disease (PD). Although dopaminergic degeneration affects a significant portion of the aging population, the pathways and mechanisms underlying it have not yet been elucidated.

The Doitsidou lab has recently established a model of dopaminergic degeneration in *Caenorhabditis elegans*. In this model, a Transient Receptor Potential (TRP) channel (TRP-4) has mutated and results in a gain of function. Based on the morphology of the dopaminergic neurons, the overactive channel is believed to be activating a necrotic cell death pathway.

This thesis aims to identify the pathways relevant to TRP-4 mediated dopaminergic degeneration in *Caenorhabditis elegans*. It takes a two-pronged approach, comparing TRP-4 degeneration to other models of neurodegeneration and conducting a forward genetic screen to identify novel candidates.

Through these approaches, the nature of TRP-4 degeneration has been further elucidated. The results gathered in this thesis explore the involvement of lysosomal acidification through the V-ATPase pump in dopaminergic cell death and are not conclusive as to whether or not the V-ATPase pump plays a role in TRP-4 induced degeneration. The lysosomal biogenesis pathway is implicated in dopaminergic degeneration in the TRP-4 model. Differences in lysosomal morphology in dopaminergic neurons are established between the wild type and degenerating states. Finally, three full and three partial suppressors of degeneration were discovered through the automated forward genetic screen. Together, this thesis brings insight into intracellular the mechanisms underlying a novel, TRP-channel based model of dopaminergic degeneration.

Acronyms

Acronym	*Meaning*
ADE	*Anterior deirid*
ASP	*Aspartyl*
ATP	*Adenosine triphosphate*
bp	*Base pairs*
CALB	*calbindin*
cDNA	*complementary deoxyribonucleic acid*
CEPD	*dorsal cephalic*
CEPV	*ventral cephalic*
CLP	*calpain*
CMA	*chaperone-mediated autophagy*
CNX	*calnexin*
CRT	*calreticulin*
CSP	*caspase*
DA	*dopaminergic*
DAT	*dopamine transporter*
DEG/ENaC	*degenerin/epithelial sodium channel*
DNA	*deoxyribonucleic acid*
ds	*Double stranded*
EGL	*egg laying defect*
EGTA	*ethylene glycol tetra acetic acid*
EMS	*Ethyl methanesulfonate*
ER	*endoplasmic reticulum*
F	*Forward*
F_1	*First filial generation*
F_2	*Second filial generation*
F_3	*Third filial generation*
GBA	*Glucocerebrosidae*
GD	*Gaucher's Disease*
GFP	*green fluorescent protein*
GLO	*Gut granule loss*
GoF	*gain of function*
GoI	*Gene of interest*
HS	*heat shock*
iPS	*Induced pluripotent stem cell*
LB	*Lewy body*
LG	*Linkage group*
LMP	*Lysosome membrane protein*
LoF	*loss of function*
LRO	*Lysosome related organelle*
NCBI	*National Center for Biotechnology Information*
NCCD	*Nomenclature Committee on Cell Death*
NGM	*Nematode growth medium*
NPG	*Nature publishing group*
P_0	*Parental generation*
PCD	*programmed cell death*
PCR	*Polymerase chain reaction*

PD	*Parkinson's Disease*
PDE	*posterior deirid*
R	*reverse*
RNA	*ribonucleic acid*
RNAi	*ribonucleic acid interference*
ROS	*reactive oxygen species*
RT	*Room temperature*
SEM	*Standard error of means*
SN	*substantia nigra*
SNCA	*synuclein*
TRP	*transient receptor potential*
UNC	*uncoordinated*
V-ATPase	*vacuolar H^+ ATPase*
WGS	*Whole genome sequencing*
WT	*Wild type*

Acknowledgements

First and foremost, I would like to thank my supervisor: Dr. Maria Doitsidou. In assembling this thesis, you treated the task as a professional and as a publication. Our ambitions were high, but thanks to your advice and extensive efforts, I am happy to put my name on this thesis. While others will be able to provide me with guidance, you will always be my mentor and I look forward to the long years of friendship and scientific breakthroughs (of course!) that await us.

Additionally, my sensor, Dr. Anders Olsen, deserves thanks. Primarily, I am grateful that he agreed to be my sensor: travel to be my opponent and determine my competency as a scientist in the context of this thesis- as well as to take the time to read and consider my thesis.

In relation to this thesis, I would like to thank my fiancé, Roberto Martín Muñoz, for his understanding and patience. He is annoyingly optimistic and never hesitated to tell me just one more time to try again or to keep going. He, without fail, would make a joke, share an article, or a picture of a cat or elephant (of which there were many!)- all to lift my spirits momentarily and keep me in check and my thoughts in perspective.

Another one to lift my spirits always was Dr. Archana Nagarajan. I thank her for being a good desk neighbor and always seeing when I needed a break- and caring that I didn't skip out on lunch to work more. Many thanks to Archana for blinding me for scorings and for providing feedback on morphological observations. Finally, we are all indebted to her for her prowess with statistics.

Dr. Janete Chung deserves almost as much credit as my own fingers for this thesis. It was thanks to Janete's generosity that my constant supply of strong 100% Brazilian coffee was never in question. Moreover, Janete engineered the screening strain used for this thesis and completed one round of screening.

I would like to acknowledge Dr. Kaja Reisner for her extensive feedback on the worm. Kaja gave me hope that spontaneous males exist and can actually be found on a regular basis. Additionally, I thank Kaja for being my bench partner and for humoring my mildly OCD organization. Kaja also deserves thanks for injecting the LMP-1 construct.

This thesis would have been on a very different level without the help of Dr. Ye Ning. I especially thank him for his help with *trp-4(d)* genotyping, teaching me DCAPs primer development and use, and for help on the LMP-1 cloning, on which he gave much needed feedback.

Special thanks to the Hermann (the *glo* allele), Jorgensen (the *vha-12* allele), and Tavernarakis (*mec-4* mutant) labs for personally sending requested alleles of strains.

I would like to thank my classmates and professors for providing me with an engaging intellectual environment here at UiS. Additionally, I would like to thank all of CORE for providing this environment as well. Special thanks to Marina, Oleg, and Jodi for their varied brands of moral (and caloric) support.

Finally, I would not be here (biologically and geographically) without the constant support and guidance of my family. Never once did they pressure me to do anything in life, and instead encouraged me to do what would fulfill me- and to explore against all my fears. They are my constant examples of what real work ethic looks like and a constant reminder of the loving support with I am blessed with.

Sincerely,
Tatiana Mikhaelovna Popovitchenko BA, (fingers crossed) MSc.

Introduction

A model of neurodegeneration: TRP-4

In an automated forward genetic screen in *Caenorhabditis elegans* for mutants involved in dopaminergic specification (Doitsidou et al., 2008), the *trp-4(ot337)* or *trp-4(d)* mutant was discovered. This mutant has a full set of DA neurons embryonically and fewer than normal in adulthood (Nagarajan et al., 2014). Using whole genome sequencing (WGS) and bioinformatics analysis software the responsible mutation was identified. The progressively degenerating mutant had an M1779I[1] amino acid substation mutation in the gene encoding TRP-4 (Nagarajan et al., 2014).

TRP-4 is part of the Transient Receptor Potential channel superfamily. It is the sole TRPN member in *C. elegans*. The TRP proteins are involved in sensation, including vision, taste, olfaction, hearing, touch, and thermo-and osmosensation. While TRPN members are present across much of phylogeny, they are not conserved in mammals- although there are at least twenty eight different TRP members found in mammals (Venkatachalam and Montell, 2007). TRP-4 coordinates as a pore-forming subunit of the mechanotransduction channel in DA neurons (Kang et al., 2010). Structurally, TRP-4 is a protein composed of: four ankyrin re-

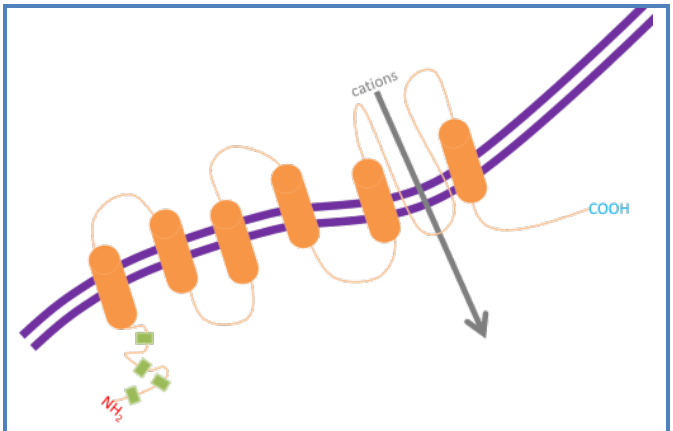

Figure 1 The TRPN channel in *C. elegans* is composed of six transmembrane segments. The amino and carboxy terminals are both intracellularly located. Cations, including Ca^{++} and Na^{+}, enter through a channel located between the fifth and sixth transmembrane segments. Four ankyrin repeats (green boxes) are located at the amino terminal. Figure adapted from (Nagarajan et al., 2014).

[1] G13503A is the nucleotide substitution

peats at the amino terminal, six transmembrane segments, a cation permeable channel between the fifth and sixth segments, and intracellular amino and carboxy terminals (**Figure 1**) (Nagarajan et al., 2014).

Phenotypically, *trp-4* null animals exhibit locomotion defects, including exaggerated bending and a distinct body posture, which suggest a stretch receptor role for the channel (Li et al., 2006). In *trp-4* loss -of-function mutants, there is no observed effect on dopaminergic neuron survival. In *trp-4(d)* mutants, there is a loss of the majority of dopaminergic neurons, suggesting that these mutants carry a gain-of-function mutation. Moreover, in *trp-4(d)* mutants the dopaminergically dependent basal slowing response behavior is lost even in worms with surviving dopaminergic neurons; which suggests that the mutation interferes with channel function (Nagarajan et al., 2014).

As the null mutant does not show DA degeneration, the dominant mutation in the *trp-4* locus was shown to be responsible for the degeneration phenotype through recapitulation[2] experiments (Nagarajan et al., 2014). *trp-4(d)* is expressed in the DA neurons, the DVA and DVC neurons (Li et al., 2006), and fourteen additional head neurons (Nagarajan et al., 2014). While a wild-type worm has eight DA neurons **Figure 2**, the phenotype of an adult *trp-4(d)* worm is severely degenerating CEPs, mildly degenerating ADEs, and non-degenerating PDEs (Nagarajan et al., 2014).

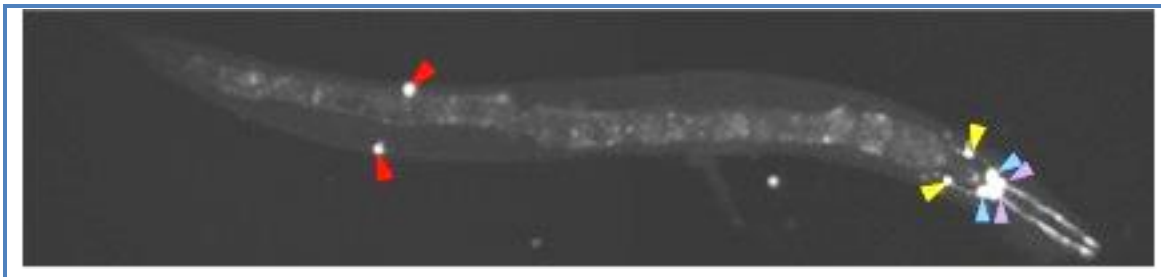

Figure 2 The DA neurons of *C. elegans* are shown here. There are two of each class: CEPVs (purple arrows), CEPDs (blue arrows), ADEs (yellow arrows), and PDEs (red arrows). The animal is shown from left to right: posterior to anterior. DA neurons are marked with a DAT-1::GFP reporter. Image credit: Maria Doitsidou.

[2] There were two proof of principle experiments: 1) a reversion of phenotype screen and 2) trp-4(ot337) cDNA introduction into the WT.

Involvement of Calcium

TRP channels are known to conduct monovalent and divalent cations such as Na^{+} and Ca^{++} (Venkatachalam and Montell, 2007) and known to be involved with intracellular Ca^{++} homeostasis (Gees et al., 2012). Ca^{++} dyshomeostasis is one of the key events in a supposed necrotic cell death pathway (Golstein and Kroemer, 2007) and is implicated in a range of neurodegenerative diseases (Galluzzi et al., 2012).

The *trp-4(d)* channel's relationship to Ca^{++} homeostasis has been genetically and pharmacologically explored. When *trp-4(d)* mutants are exposed to calcium-chelating factors, such as the chemical EGTA or when calbindin (calcium-binding protein) is expressed in the dopamine neurons of these mutants, degeneration is suppressed. *trp-4(d)* has also been crossed with calreticulin, a Ca^{++} binding ER chaperone, and consequently showed significant decrease of degeneration. ER Ca^{++} exit has been blocked with dantrolene and again suppression was observed (Nagarajan et al., 2014). Thus, Ca^{++} homeostasis was previously shown to be a key contributor to DA degeneration in the *trp-4(d)* model.

Mode of cell death

Determining the mode of cell death at play in *trp-4(d)* induced degeneration is not a facile task. While there is an established canonical apoptotic pathway, no such certainty exists for necrosis. Although morphological data alone is no basis for conclusion, it does provide a key insight into the mode of cell death. *trp-4(d)* degeneration is seen in **Figure 3** and exhibits characteristic rounded necrotic morphology (Nagarajan et al., 2014).

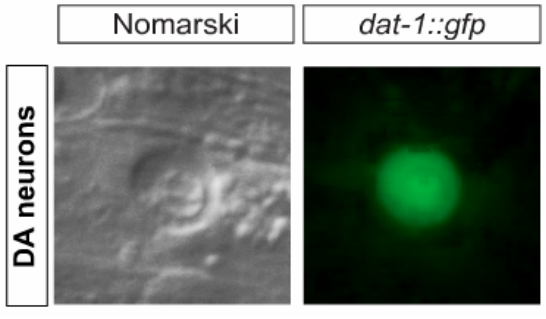

Figure 3 *trp-4(d)* degeneration in a DA neuron. While neurons are typically elongated, the DA neuron here is uncharacteristically rounded in shape. From *Figure 3* in (Nagarajan et al., 2014) **.**

Previously, in order to ascertain whether or not the death occurring in the *trp-4(d)* model was apoptotic, var-

ious factors in the well-established apoptotic pathway in *C. elegans* (**Pathway 1**) were genetically explored. Specifically, the executioners of apoptosis *ced-3* and *ced-4* have been tested in the *trp-4(d)* model and were all found not to be involved. Additionally, non-canonical apoptosis *C. elegans* caspases (*csp-1, csp-2, csp-3*)[3] were tested and also found to be dispensable to the *trp-4(d)* model of cell death (Bachelor's Thesis, Strenitz, 2014) (Nagarajan et al., 2014).

egl-1 ⊣ ced-9 ⊣ ced-4 → ced-3 Pathway 1

Great strides have been taken to determine the identity of a necrotic pathway; this too is on its way to being defined with the help of the model nematode. Studies from the Tavernarakis and Driscoll labs have pioneered the exploration of necrotic mechanisms in *C. elegans*. Though necrosis has no defined pathway or classical understanding like apoptosis, thanks to the work done in these and other labs there are several events associated with necrosis. These events include: Ca^{++} dyshomeostasis, requirement of calpains and cathepsins, and lysosomal alteration (Golstein and Kroemer, 2007). Despite this, the list of necrotic events is not definitive and a canonical necrotic pathway is still open for further characterization.

A key event in proposed necrotic pathways is the activation of aspartyl and calpain proteases (**Figure 4**). Syntichaki *et al.* proved their necessity for death in the *mec-4(d)* model (Syntichaki et al., 2002). Calpain[4] and aspartyl proteases were tested in this lab with single-gene knockdowns for involvement in *trp-4(d)* cell death and found to be uninvolved. The aspartyl proteases ASP-1, ASP-3, ASP-4[5], and ASP-5 were tested with RNAi experiments and similarly showed no effect (Bachelor's Thesis, Maugard, 2013). However, it is possible that redundancy is-

[3] It should be noted that for *ced-9, csp-1, csp-2,* and *csp-3* there was an insufficient sampling of the population (<50 individuals). However, general trends were established that can be considered in the context of the remaining significant results.
[4] With crossing (*clp-2, clp-4, clp-6,* and *clp-7*) and RNAi (CLP-1, CLP-4, and TRA-3).
[5] Recently crossed and again found to be irrelevant.

sues might be responsible for the absence of observed effects of these cases on the dopaminergic degeneration in the *trp-4(d)* model.

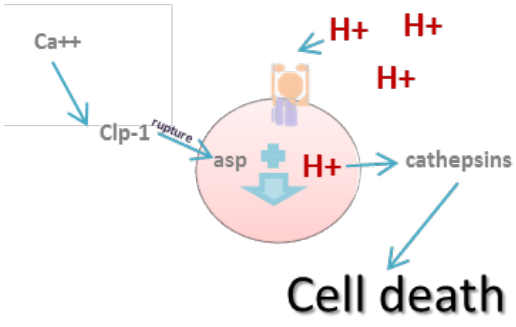

Figure 4 The Calpain/Aspartyl pathway in necrosis is shown here. Calcium ions activate calpain proteases, which normally cleave aspartyl proteases at cysteine, and abnormally rupture the lysosomal membrane. The aspartyl proteases activate cathepsins. Aspartyl proteases are also notably activated by a decrease in pH, driven by V-ATPase acidification.

Although calpain and aspartyl proteases have not yet been implicated in *trp-4(d)* degeneration, the necrotic morphology, in combination with the partial suppression of degeneration in calreticulin loss of function mutants, points to a necrotic mechanism.

One recent series of experiments has identified that autophagic mechanisms are involved in *trp-4(d)*. UNC-51 activates vesicle nucleation and consequently formation of the phagophore, an important initiation step for autophagy. *unc-51* alleles and also *atg-18* alleles (a molecular player important for protein retrieval step in autophagy) were found to significantly suppress DA degeneration in *trp-4(d)* (Bachelor's Thesis, Håland, 2014).

While the autophagy results do not offer a conclusive death pathway, they do implicate an intriguing player: the lysosome. The autophagosome eventually fuses with the lysosome, thus implicating the lysosome as a downstream player in the *trp-4(d)* cell death pathway.

Structure and aim of the thesis

The aim of this thesis is to assess the role and molecular pathways that mediate dopaminergic cell death in the *trp-4 (ot337)* model. To tackle this question, a two-pronged approach has been taken; the first prong of which is the classical ''candidate'' approach. The candidate approach is often used in genetic studies and involves picking a handful of molecular targets, ''candidates,'' that have been

previously shown to be instrumental in the same or comparable pathway. The second prong of the thesis utilizes an ‘‘unbiased’’ approach and results in the identification of novel players. The approach is unbiased in that it does not anticipate a molecular player, but rather isolates one phenotypically through a genetic screen and *then* identifies it. *trp-4 (ot337)* itself was isolated and identified as part of a screen for dopaminergic fate.

Candidate Approach

The candidate chosen for this thesis have all been previously identified to be involved in the *mec-4(d)* model of necrotic cell death. MEC-4 is an overactive degenerin/epithelial sodium channel (DEG/ENaC). The mutated version causes severe and early degeneration of mechanosensory neurons. The channel was discovered by Driscoll and Chalfie and is part of the degenerin gene family, which is conserved across phylogeny (Driscoll and Chalfie, 1991) (Hong and Driscoll, 1994). It conducts excessive sodium and calcium into neurons and its actions can be suppressed by preventing release of Ca^{++} from ER channels or storage of Ca^{++} within the ER, such as in calreticulin mutants (Bianchi et al., 2004) (Xu et al., 2001). Previous studies exploring neuroprotective factors in *mec-4(d)* induced neurodegeneration have implicated several necessary agents for the necrotic pathway, among them: the vacuolar H^{+}-ATPase (V-ATPase) pump, the hormeotic protection of moderate heat shock, and the biogenesis of the lysosome. In this thesis, we explored these neuroprotective factors for their ability to ameliorate *trp-4(d)* dopaminergic degeneration. The candidate pathways that will be explored in this thesis are graphically summarized in **Figure 5**.

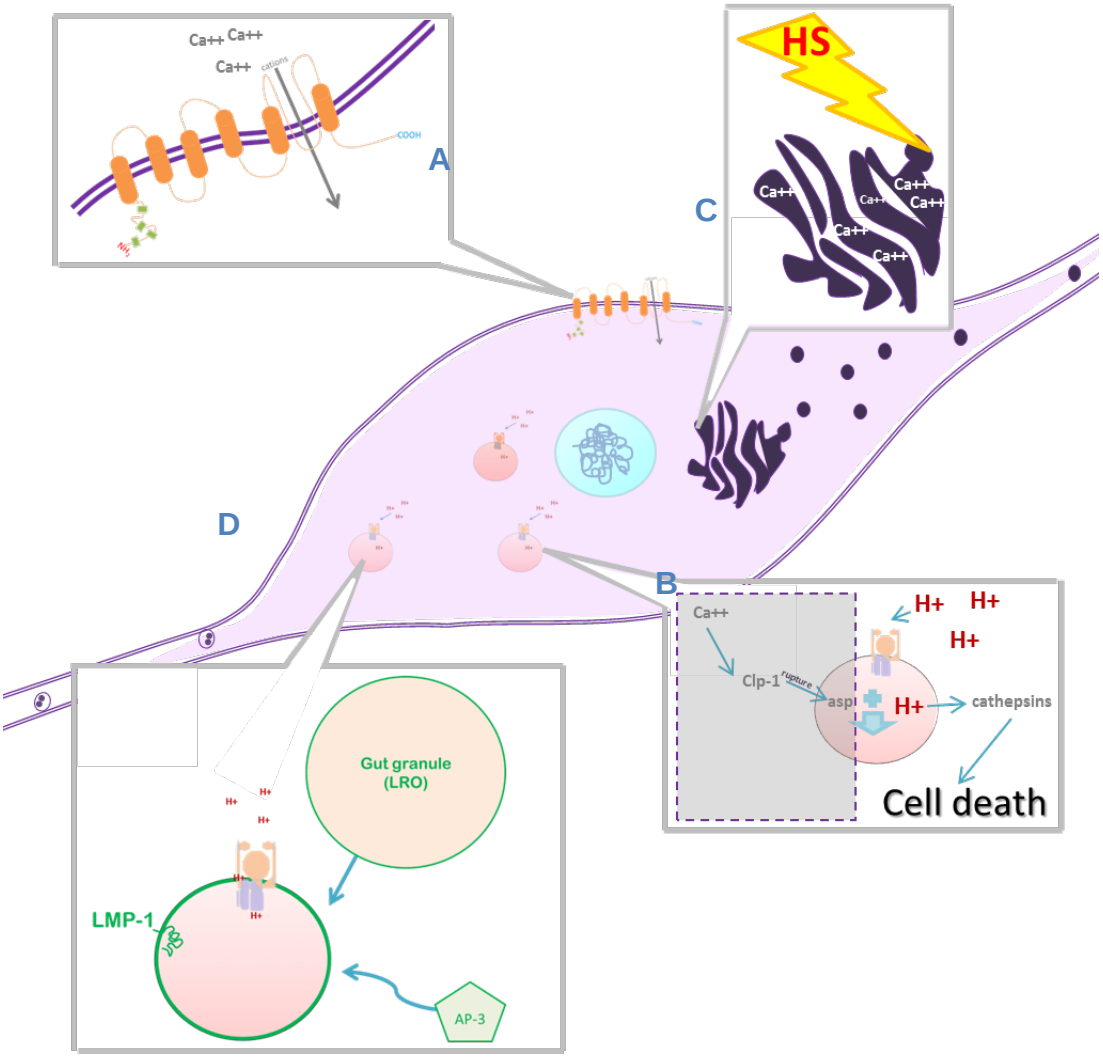

Figure 5 Pathways explored during the Candidate Approach includes various strategies aimed at identifying the pathways that mediate *trp-4(d)* induced degeneration.. The entire illustration is of a generalized *C. elegans* dopaminergic neuron. **A** shows the *trp-4* channel, with transmembrane domains and intracellular amino and carboxy terminals. Figure adapted from (Nagarajan et al., 2014). **B** shows the V-ATPase pump present on the lysosomal membrane with protons entering into the cell through the pump and activating the release of the cathepsins. (In the grey box rests a pathway –not tested in this thesis- in which Ca^{++} activated calpains rupture the lysosome, unleashing the aspartyl proteases and ultimately lead to cell death). **C** illustrates the Golgi body with internal Ca^{++} stores. With Ca^{++} being buffered by the Golgi after preconditioning (HS thunderbolt in the schematic), the cell may be more resilient even with excitotoxic influx of Ca^{++} (**A**). **D** depicts lysosomal biogenesis.

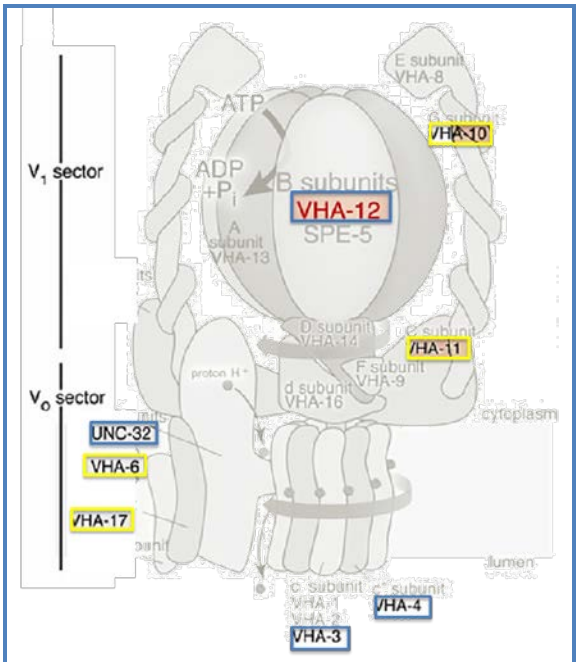

Figure 6 The V-ATPase pump sits on the membrane of organelles. It consists of two sectors: V_1 and V_0. The V_1 sector is membrane bound and contains the major B subunit. The V_0 sector is cytoplasmically located and regulates the flow of protons into the lumen of the lysosome. Blue and yellow boxes are indicative of experiments performed for this thesis. Figure is adapted from (Ernstrom et al., 2012).

Vacuolar H^+ ATPase Pump

This thesis primarily focuses on the involvement of the lysosome in the *trp-4(d)* model of degeneration. Lysosomal acidification is a key event in previously described necrotic pathways (Artal-Sanz et al., 2006) To test the acidification theory this thesis explores, in the context of *trp-4(d)* model, the role of the V-ATPase pump, a factor in lysosomal and cellular pH (Syntichaki et al., 2005).

The V-ATPase pump (**Figure 6**) that rests on the membrane of organelles is responsible for the acidification of the lysosome at the cost of one molecule of ATP. ATP is hydrolyzed to ADP by the major B subunit of the pump, controlled by genes *vha-12* and *spe-5*. The D subunit twists to begin the mechanism of lysosomal acidification. Ultimately, the c and c^+ subunits will direct the flow of protons into the lumen of the lysosome. The pump is functional in acidification of synaptic vesicles, regulation of neurotransmitter release, embryogenesis, zygotic morphogenesis, and apoptotic- corpse clearance (Ernstrom et al., 2012).

Additionally, the V-ATPase pump has been implicated in necrosis. *vha-2*, *vha-10*, and *vha-12* were tested in *mec-4(d)* mutants and were found to ameliorate cell death in the six *C. elegans* mechanosensory neurons. *vha-12* showed the strongest suppression of all (84%) when mutated in the *mec-4(d)* mutant[6]. Lyso-

[6] *Mec-4(d)* had about 220/600 vacuolated cells and *mec-4(d)*;vha-12(n2915) had about 90/600 vacuolated cells, **Figure 1A** in *Syntichaki, P., Samara, C. and Tavernarakis, N. (2005) 'The vacuolar H+ -ATPase mediates intracellular acidification required for neurodegeneration in C. elegans', Curr Biol, 15(13), pp. 1249-54.*

somal acidification is crucial to the necrotic mechanism. Sharp decrease of the acid-base balance in the lysosome triggers aspartyl[7] proteases to release digestive cathepsin enzymes into the cell. Cellular acidification is regulated by the V-ATPase pump and it has been suggested that necrotic cells demonstrate a lower cytoplasmic pH (Syntichaki et al., 2005) (Syntichaki and Tavernarakis, 2003).

The involvement of the V-ATPase pump in dopaminergic degeneration was tested in this thesis **genetically** with crosses (blue boxes in **Figure 6**) and RNAi (yellow boxes in **Figure 6**), and **pharmacologically** with the bafilomycin chemical.

Lysosomal biogenesis

Lysosomal biogenesis refers to the generation of new lysosomes in the cell. Pathways that transport lysosomal membrane proteins and pathways that transport hydrolases to the lysosome are both considered part of lysosomal biogenesis. As the lysosome is the ultimate site of all cellular degradation, it is inherently a suspect in cell death pathways. Indeed, lysosome morphology was previously shown to be altered during necrotic cell death and lysosomal biogenesis was found to contribute to *mec-4(d)* induced necrosis (Artal-Sanz et al., 2006).

In order to morphologically assess the effect of *Trp-4(d)* channel on lysosomal morphology, a lysosomal associated membrane GFP fusion protein (LMP-1::GFP) under the dopaminergic DAT-1 promoter was cloned and subsequently injected into *trp-4(ot337)* animals (**Figure 5D**). By comparing the LMP-1::GFP in mutant and wild-type animals, morphological observations concerning the consequences of *trp-4(d)* mutation on lysosomal morphology.

In *C. elegans*, a Rab GTPase called GLO-1 is required for the biogenesis of lysosome related organelles (LRO) called gut granules. They are known to be in the gut (Hermann et al., 2005), but their presence has not been determined in the DA neurons. They are typically larger than lysosomes and are thought to be a storage related organelle; particularly zinc storage (Coburn and Gems, 2013). *glo* mutants were shown to be defective in lysosomal biogenesis and their absence

has been shown to be a protective effect in mechanosensory neurons in the *mec-4(d)* model. (Artal-Sanz et al., 2006).

Since lysosomal morphology and biogenesis were affected in the *mec-4(d)* mutant, these two points will be tested in this thesis. Morphology will be explored with the use of a lysosomal reporter and biogenesis with genetic candidates.

Heat shock preconditioning

One pathway that was shown to be relevant in preventing several types of necrotic cell death involves heat shock preconditioning. Preconditioning is a kind of adaptation. Stress can happen in extreme amounts, such as the kind caused by *trp-4(d)* channels, or in small amounts. It has been shown that small and slow exposure to stress may better prepare a system for larger onslaughts (Calabrese, 2004).

Stressors are diverse and can take various forms including heat and hypoxia. By exposing *C. elegans* to extreme and less extreme heat, one can test the hormetic theory. This was indeed previously employed in the case of necrotic cell death, and it was observed that heat shock induced necrosis was limited after moderate heat preconditioning. Furthermore, preconditioning had a protective effect in both the *mec-4(d)* model and a PD α-synuclein model of cell death. This suggests that the protection provided by the heat-shock-response pathway is wide-ranging and not exclusive to one type of stressor (Kourtis et al., 2012).

In the *mec-4(d)* model it was shown how preconditioning affected a cell undergoing necrotic insults: It sequestered cytoplasmic Ca^{++} increase caused by necrotic insults by increasing Ca^{++} uptake by the Golgi apparatus. (Kourtis et al., 2012).In this thesis, similar experiments were conducted to see what effect preconditioning has on *trp-4(d)* induced damage (**Figure 5C**).

Unbiased approach

C. elegans is an excellent organism to perform forward genetic screens with because of its versatility (Tucci et al., 2011). Suppressors for *mec-4(d)* induced degeneration were discovered through this kind of screen (Xu et al., 2001). While in

the mec-4 screen, worm coordination was used as a selecting factor, for this thesis, GFP brightness was the selecting factor. The same method and approach were taken in a screen conducted in the Hobert lab for dopaminergic specification (Doitsidou et al., 2008). It was during this screen that two trp-4 mutant alleles were discovered, one of which was *ot337*, the gain-of-function allele used for this thesis .

A previous *trp-4(d)* suppressor screen in the Doitsidou lab, yielded many intragenic suppressors. In this thesis, a strain with two copies of *trp-4(ot337),* one endogenous and one engineered into the *C. elegans* genome is used. In order to discover novel factors in *trp-4(d)* pathways, a forward genetic screen was performed on this newly engineered screening strain.

In summary, by way of the *trp-4(d)* model, this thesis aims to address both morphological and biochemical aspects of cell death. This is to be done with a two-pronged approach: candidate and unbiased. *trp-4* is remarkable for the fact that it is a progressive and robust death model. Though models will always be imperfect, the *trp-4* mutant allows us an entry point into a novel understanding of dopaminergic degeneration.

Theory

Parkinson's and Dopaminergic Degeneration

An historic overview

In 1817, in *An Essay on the Shaking Palsy*, James Parkinson detailed the manifestation of paralysis agitans in his patients, as well as in random passersby on the street. So characteristic is the disorder that three out of six described cases were purely observational and took place at a distance. Today, mostly in honor of his thoroughness of description and of his efforts to make a unifying definition of the disease, paralysis agitans is known as Parkinson's Disease (PD) (Parkinson, 1817).

In 1919, proof arose for the origins of PD that separated it from other brain disorders. It was in that year that Konstantin Tretiakoff defended his thesis[8] at the University of Paris. In his examination of the substantia nigras (SN) (blue box and line in **Figure 7**) of nine brains from patients suffering paralysis agitans, Tretiakoff noticed a, ''marked loss of the pigmented nigral neurons with swelling of cell bodies, [granular] degeneration and neurofibrillary alterations.'' Tretiakoff noticed another irregularity in the SNs of the affected brains and named them ''corps de Lewy,'' or, Lewy bodies (LBs). Even today, the identification of LBs in the SN of patients is a key diagnostic tool for clinicians. Tretiakoff observed these findings in not only Parkinsonism cases, but also other disorders in which muscular tone was affected[9] and they were further supported with more brain dissections.

[8] *A Study of the Pathological anatomy of the locus niger of Soemerring and its relevance to the pathogenesis of changes in muscular tone in Parkinson's Disease*. NB: the *locus niger of Soemerring* is the substantia nigra.

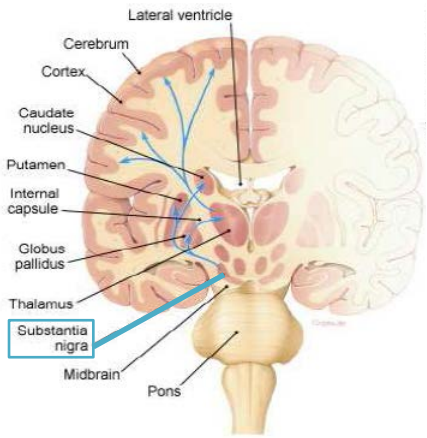

Figure 7 Coronal view of the human brain. The blue arrows demonstrate the dopaminergic innervation that begins in the substantia nigra and flows throughout the basal ganglia and eventually into the cortex. PD degeneration occurs in the substantia nigra (SN) (containing the substantia pars compacts and the substantia nigra reticulate), which, along with the striatum (the caudate and putamen nuclei), Globus pallidus, and the subthalamic nucleus make up the basal ganglia- the region of the brain associated with voluntary motor control.

The thesis did not spur scientific exploration into the curious loss of pigmented neurons from the SN and the appearance of the strange LBs. Yet, this should not be surprising, as the SN is not the only affected brain region in PD. Though it is the first hit, the loss of neurons there will cause a denervation in the regions that the projections normally reach. The general pathways of these projections are shown in **Figure 7**. Though it was Tretiakoff that identified the LBs in the SN and the loss of pigmented neurons from the SN (also confirmed by Hassler in 1938), it would take some more scientists and decades to identify what those pigmented neurons were and why their loss was so devastating.

The SN is a relatively easy area of the brain to identify, due to the pigmented neuromelanin[10] containing dopaminergic neurons (Fedorow, Tribl et al. 2005). The distribution of dopamine in the dog brain was demonstrated by Bertler and Rosengren in 1959; weeks later, also shown by Sano in the human brain. It was Hornykiewicz that uncovered the loss of DA neurons from the substantia nigra, when he characterized dopamine in Parkinsonian[11] brains (Fedorow et al., 2005). With these discoveries, the pathological understanding of PD was extended, and its treatment became a reality with the administration of L-Dopa. However, what remained to be understood was why the DA cells were dying in the first place.

[10] Neuromelanin is thought to be a byproduct of oxidative polymerization of both the catecholines dopamine and noradrenaline

Molecular insights

The discovery of monogenic forms of PD heralded in a new age of PD research: one of mechanisms. Once the genetic players are identified, and proteins are consequently implicated, researchers can explore these molecules and what pathways they take part in.

Several genetic loci have been identified in the recent years to be causal to PD, and their study gave us insights into mechanisms. It was shown that **PINK-1** and **Parkin** a) interact with each other, b) are in the same pathway with Parkin as the downstream player, and c) are both involved in mitochondrial health in muscle and dopaminergic cells (Yang et al., 2006, Park et al., 2006, Clark et al., 2006). Another recent study proved the suspected mechanistic link between Glucocerebrosidase (GBA) and **α-synuclein.** The group determined that this interaction created a destructive feedback loop that resulted in increased aggregations of α-synuclein in the lysosome and eventually neurodegeneration (Mazzulli et al., 2011).

The lysosome in particular has been getting much attention in PD research. It is the site of all degradation in the cell and along with such mechanisms as chaperone-mediated autophagy (CMA) can specifically target harmful structures to the cell. α-synuclein is normally degraded in the lysosome. However, when α-synuclein begins to aggregate, it becomes insoluble in this environment. Macroautophagy can to some extent deal with these large oligomers, but not beyond the point where the aggregates become toxic. The oligomers will eventually interfere with lysosomal membrane integrity. The A53T mutation in α-synuclein exacerbates matters by interfering with CMA. Additionally, the PD mutation in LRRK2 has been associated with impaired autophagy; as have mutations in PINK1 and Parkin in the mitochondria, leading to impaired mitophagy (autophagy of mitochondria) (Dehay et al., 2013).

Despite the identified genetic causes of PD and the numerous mechanistic insights their study provided, the precise molecular mechanisms that lead to do-

paminergic degeneration in the SN are not yet fully understood, which is reflected in the lack of successful therapeutic interventions for PD.

Cell death

In seeking to further understand neurodegenerative diseases like Parkinson's, it is imperative to develop knowledge in the area of cell death mechanisms. Cell death occurs both naturally, for example in digitation of fingers and human brain development or pathologically, like in the case neurodegenerative diseases. Various cell death pathways are outlined in **Figure 8**.

General Overview

There are three classical archetypes of cell death: apoptosis, autophagy, and necrosis. They have all been described in literature and are respectively known as types I, II, and III[12] (Kerr et al., 1972). However, many researchers dichotomize cell death into apoptosis or necrosis. In this approach, apoptosis involves **caspases**, and is **non-immunogenic** and **programmed** versus necrosis which does not involve caspases and is immunogenic and pathological (Galluzzi et al., 2012).

Caspases are proteases that activate the apoptotic execution pathway (Black et al., 1988). The resulting cell death generally does not activate an external **immune** response -in contrast with necrosis. During necrosis, cells swell in size along with their organelles and eventually the plasma membrane will burst. Intracellular contents will be exposed to the extracellular environment, ultimately triggering an inflammatory response and exposing the neighboring cells to stress

[12] The use of these labels (Type I etc.) has been discouraged by the NCCD in light of growing evidence that cell death molecules are active in more than one pathway and can be repurposed- making the lines between the mechanisms less distinct.

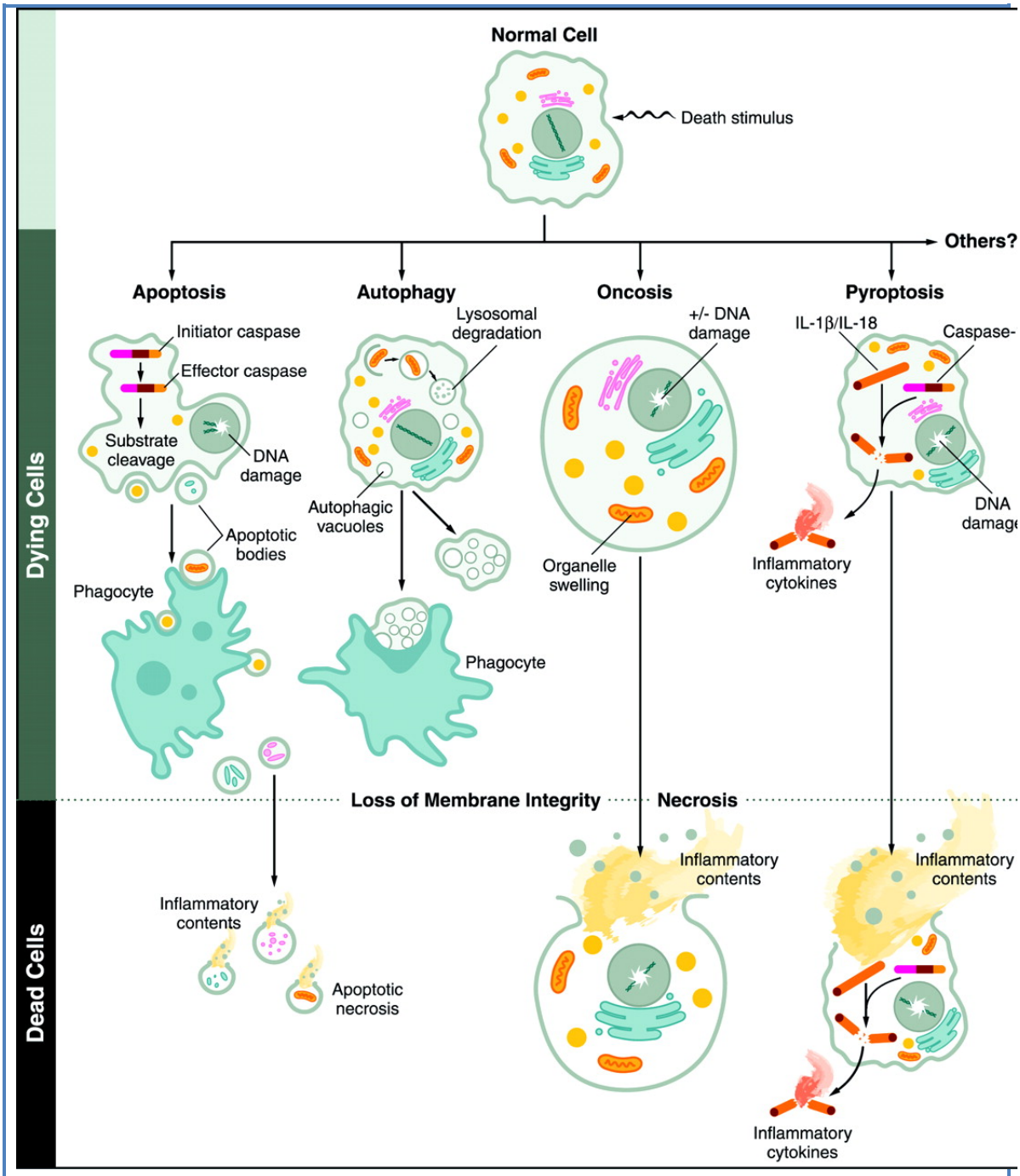

Figure 8 Morphological contrast of apoptosis and necrosis from (Fink and Cookson, 2005). Oncosis refers to a gain in cell volume- in this image it is depicted as a form of necrosis. Pyroptosis is a caspase-dependent cell death pathway-however is also proinflammatory, thus putting it on the side of necrosis. This figure demonstrates the level of flexibility necessary in considering the various cell death modalities.

and toxicity (Raff, 1992) (Kerr et al., 1972).

Yet, the clear contrast of apoptosis versus necrosis is not without its caveats. **Caspase**-independent forms of apoptosis have been described. Apoptosis can occur via three different pathways: extrinsic (death receptor based), intrinsic (mitochondria based)[13], and granzyme induced (Elmore, 2007). Although apoptosis was first described by Kerr as ''shrinking necrosis,'' now that it has been molecularly characterized the tables have turned and necrosis is defined in the negative: as not involving apoptotic or autophagic markers (Kroemer et al., 2009). Apoptosis can be controlled and prevented, and is a form of Programmed Cell Death (PCD) (Lockshin and Williams, 1965). It is often contrasted with necrosis in its utilization of built-in cell machinery. The characterization of necrosis as ''accidental'' or **unprogrammed** has been falling out of favor. In fact, it has been suggested that various necrotic hallmarks have been evolutionarily conserved and are thus part of the essential cell machinery. In their review of molecular necrosis, Golstein and Kroemer compared necrotic cell death in six model systems[14] and compiled a list of common features in the necrotic death program:

- Mitochondrial dysfunction and swelling
- Reactive oxygen species (ROS) production
- ATP depletion[15]
- Ca^{++} dyshomeostasis
- Perinuclear clustering of organelles
- Activation of proteases (calpains and cathepsins)
- Lysosomal rupture
- Plasma membrane rupture

It should be stated that not one model organism or system showed evidence of all of these features. The exact events of the necrotic death pathway seem to be

[13] The distinction between extrinsic and intrinsic is not rigid, and molecules from either pathway can influence each other (Igney and Krammer 2002).
[14] The systems and their inducers (in parentheses): L929 (Tumour Necrosis Factor), primate neuronal cells (ischemia), rabbit kidney cells (antimycinA), human T cell lines (Anti-Fas and others), *C. elegans* neuronal cells (mec-4(d) and others), and *D. discoideum* (dev. signals in *atg*$^{-}$ mutants).
[15] A crucial distinction between apoptosis and necrosis is ATP utilization. In necrosis, ATP is characteristically reduced and in apoptosis, it is increased in order to carry out the classical mechanism.

dependent on mode of activation (Golstein and Kroemer, 2007) or require a more stringent and biochemical characterization of the necrotic event, per the updated NCCD guidelines (Galluzzi et al., 2012). The attempt to unify the observed necrotic events into a single cohesive pathway has not reached a point where it is consistently reproducible or conserved. Its failure exposes the need for increased study of cell death and possibly an acceptance that the cell death pathways are homeostatically complex. There is a mix of pro-death and pro-survival pathways in the cell and levels of stress will influence the crosstalk between them (Raff, 1992). Additionally, it has been seen that in some cases if one pathway is inhibited, the cell can switch to one of the other pathways (Nicotera and Melino, 2004).

Autophagy involves the formation of autophagosomes that fuse with lysosomes and initiate degradation of intracellular material. There are three types of autophagy and they are characterized by the method of content delivery: macroautophagy, microautophagy, and chaperone-mediated autophagy (CMA). Though the specificity of autophagy is in question, recent studies have shown that the autophagosome does distinguish amongst healthy and dysfunctional components in the cell, and can contribute to pro-survival mechanisms. However, too much activation of the macroautophagy machinery can either trigger apoptotic mechanisms or engage in excessive and terminal autophagy (Klionsky, 2007). Levine and Kroemer propose that with the current evidence available it is impossible to call autophagy a ‘’*bona fide* killing event.’’ Rather, they suggest that autophagy is merely involved in the upstream events of both apoptosis and necrosis. Thus, the dichotomization of cell death into apoptosis or necrosis is an appropriate move (Kroemer and Levine, 2008). Importantly, if autophagy machinery is interfered with, cell death events increase.

The study of cell death has gone through many paradigm shifts and as such has accumulated terminology (Kroemer and Levine, 2008). Yet, it is no mystery why this problem exists. As the cell death pathways are only partially defined (excepting apoptosis), scientists observe death events that embody characteristics of many pathways and give them distinct names, although these pathways might

not reflect standalone cell death mechanisms. Some examples of these are: mitotic catastrophe, anoikis, excitotoxicity, Wallerian degeneration[16], paraptosis, pyroptosis, pyronecrosis, and entosis. To address these concerns, the Nomenclature Committee on Cell Death (NCCD) was formed[17]. It strives to establish ''non rigid and yet uniform'' guidelines in the description and characterization of cell death to move cell death research forward from a morphological basis to a biochemical one (Galluzzi et al., 2012, Kroemer et al., 2009).

Neuronal death

Neurons are no strangers to cell death. In fact, apoptosis is a necessary step in brain development. By birth, only 10% of neurons remain in the brain because during brain development many more neurons are differentiated than required. From this pool of neurons, only the ones that can form strong synapses and properly follow neurotrophic and semaphore signals are "deemed worthy"- the others ''commit suicide'' by undergoing apoptosis.

Besides developmental cell death, neurons are also prone to pathological cell death, commonly via neurodegenerative disorders. As excitable cells, neurons are prone to aberrant excitation. Imbalances in intracellular homeostatic pathways, like oxidative stress, mitochondrial dysfunction and calcium overload the cell and can mobilize apoptotic and necrotic cell death mechanisms that result in neurodegeneration (Mehta et al., 2013). Further, there is another mechanism of death peculiar to neurons. This mechanism, Wallerian degeneration, involves the death of axons, but not of the cell body. In studies of the Wld^S protein, which is responsible for carrying out the axonal degeneration, knockout results in axonal protection, but not soma protection (Conforti et al., 2007). In some neurodegenerative disorders like Parkinson's disease, there is a theme of how neurons die: axons first then cell bodies (Chu et al., 2012).

[16] Wallerian degeneration, or the death of axons, is indeed a distinct event- however- it is not a cell death mechanism, as the death of an axon is not preclusive to the death of the soma.
[17] The NCCD was formed from Nature Publishing Group's journal *Cell Death and Differentiation* and published recommendations in 2005, 2009, and most recently in 2012.

C. elegans as a model to study DA degeneration

It was in *C. elegans* that apoptosis was worked out by Sulston and Horvitz. By laboriously documenting the lineage of all the organism's cells, they were able to show that approximately 13% of somatic cells in the embryo die predictably. With this, they opened the door to a genetic basis of cell death and consequently to its mechanistic study and understanding (Lockshin and Zakeri, 2001). The impact of work done in *C. elegans* research cannot be overstated and it has been a crucial player in scientific discovery. Sydney Brenner, the founder of the field, jokingly said in his 2002 Nobel lecture that, ''without doubt the fourth winner of the Nobel prize this year is *Caenohabditis elegans* it deserves all of the honour but, of course, it will not be able to share the monetary award.'' Five *C. elegans* scientists have received three Nobel prizes since the beginning of this century[18].

C. elegans was the first organism for which there was a completed ''connectome,'' the entire nervous system wiring map. While it does not have a brain, the worm does have a nerve ring and exactly 302 neurons in the hermaphrodite's nervous system. Among its 302 neurons, there are eight dopaminergic (DA) neurons, illustrated in **Figure 9A**, that exist in four pairs; two each of: ventral cephalic (CEPVs), dorsal cephalic (CEPDs), anterior deirid (ADEs), and posterior deirid (PDEs) (Sulston and Horvitz, 1977). Current estimates of human DA neurons are in the ballpark of 500,000 (Bjorklund and Dunnett, 2007). Though there is a large quantitative gap between eight and 500,000, functionally speaking, dopaminergic neurons in *C. elegans* and humans are comparable. **Figure 9B** shows the synthesis pathway of DA in a generic neuron and synapse, and demonstrates the strong conservation of this basic pathway between *C. elegans* and humans.

[18] **2002**: Brenner, Horvitz, and Sulston for the genetics of organogenesis and programmed cell death; **2006**: Fire and Mello for work on RNA interference (RNAi); and **2008**: Chalfie for green fluorescent protein (GFP).

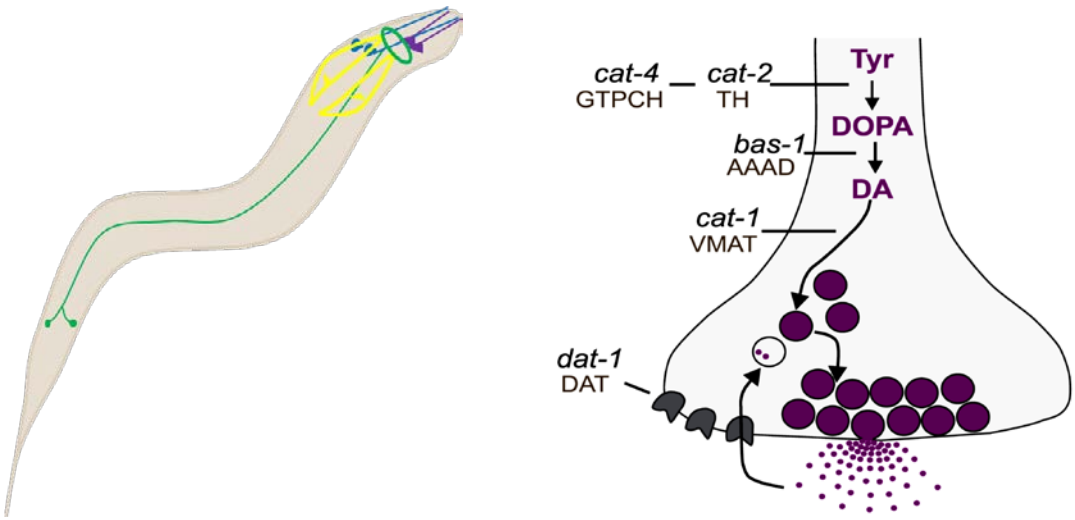

Figure 9 **Dopaminergic (DA) neurons in *C. elegans*** exist in 4 symmetrical pairs, seen in **A**: CEPVs (purple), CEPDs (blue), ADEs (yellow), and PDEs (green). The nerve ring is also shown in green. The ADEs, PDEs, and CEPDs are part of the nerve ring's innervation. **B** shows the dopamine pathway genes and conserved orthologs in C. elegans (gene on top and bolded) (Doitsidou et al., 2013).

Another strong point of conservation between humans and C. elegans is within PD genetics. Orthologs of human PARK genes are found in the C. elegans genome *C. elegans* (Dexter et al., 2012). One important gene in neurodegenerative disease not conserved in humans and nematodes is α-synuclein. However, using microinjection or bombardment, transgenic lines may be easily generated in *C. elegans* (Tucci et al., 2011). Thus, human α-synuclein was introduced into *C. elegans*. Remarkably, the overexpression of wild type or mutant α-synuclein resulted in neuronal degeneration. This result elucidated some mechanisms of α-synuclein toxicity (Lakso et al., 2003). On one hand, this is not a directly applicable result in humans. The α-synuclein protein in this case is foreign. On the other, one can observe the exact actions of the protein, mutant and wildtype, without interference from the endogenous copy (Dexter et al., 2012).

C. elegans is an ideal model organism for basic research within neuroscience. As Brenner said, ''So genocentric has modern biology become that we have forgotten that the real units of function and structure in an organism are cells and not

genes'' (Brenner, 2003). Because of its transparency, expression of GFP-tagged proteins can be observed *in vivo*. Gene knockdown is made simple with RNAi and knockouts are available almost genome wide in *C. elegans*. Nature can be manipulated and observed in this organism. Moreover, though simple, its cellular machinery is comparable to that of humans. Its simplicity is indeed an advantage in the case of the nervous system. Establishing basic mechanisms in *C. elegans'* dopaminergic neurons will lead to building the foundation for understanding equivalent mechanisms in humans.

Basic *C. elegans* biology

C. elegans has a predictable and short lifecycle, producing progeny within approximately three days at 25º, four days at 20º, and three days at 15º (**Figure 10** for the standard 25º lifecycle).

C. elegans is a dioecious species: consisting of a hermaphrodite, five autosomes and two sex chromosomes (XX), and a male, five autosomes and one sex chromosome (XO) (Herman, 2005) (Pictured in **Figure 10B**). Hermaphrodites can be singled to plates and will self-fertilize. Genetic crosses in *C. elegans* depend on the preferential use of the male sperm to the hermaphrodite's own sperm. Male sperm is larger and can crawl faster (Singson et al., 1999).

However, males occur one out of every five hundred animals in WT population. Males are the result of an X chromosome non-disjunction event during meiosis. A male, if crossed with a hermaphrodite, will result in a population with 50% occurance of the event, a 50/50 male/hermaphrodite population; if one spontaneous male is found it can be mated with a hermaphrodite to produce a male-enriched population. Alternatively, a high incidence of male (*him*) strain can be used, Finally, the event can be induced with heat shock (Hodgkin et al., 1979).

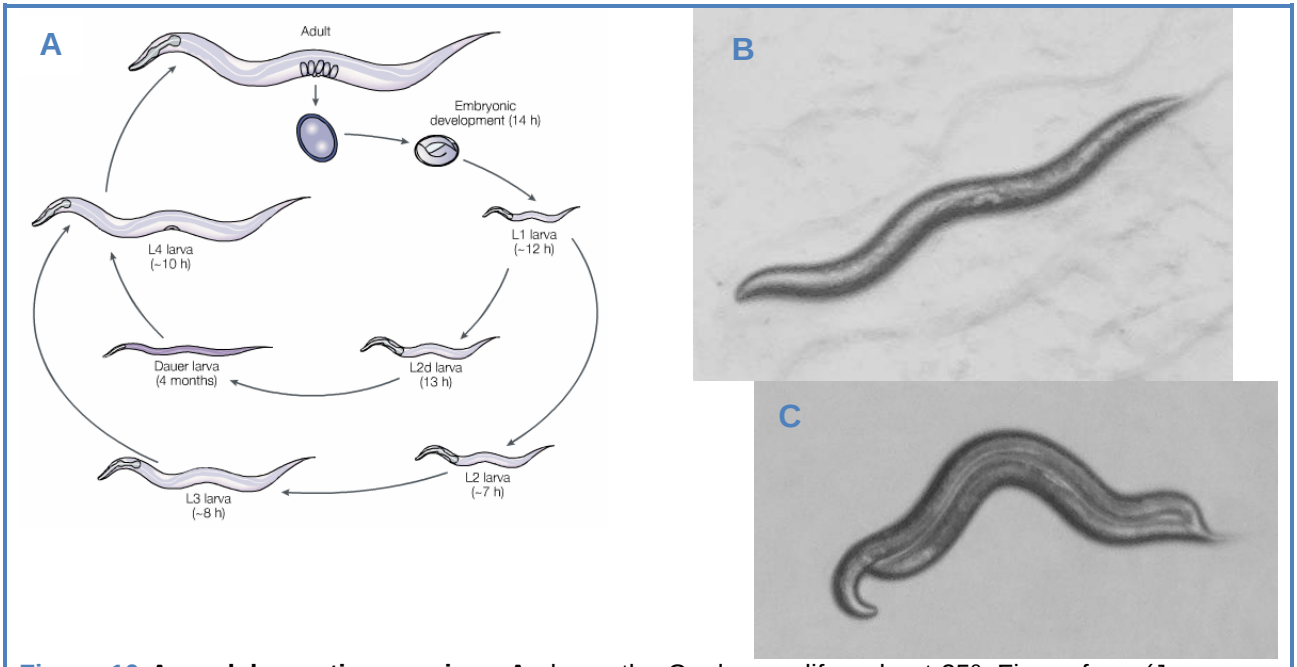

Figure 10 **A model genetic organism. A** shows the C. elegans lifecycle at 25º. Figure from (Jorgensen and Mango, 2002). **B** and **C** refer to Crossing C. elegans. In **A** the L4 life stage is shown, characterized by the half-moon shape in the middle of the worm. For mating, a worm slightly older should be selected, as seen in **B.** The male is superiorly located in relation to the hermaphrodite. Images were taken by the author with an iPhone 5 camera and on a dissecting scope.

Experimental Methods

C. elegans

Standard *C. elegans* care and maintenance was followed for this thesis as previously described (Brenner, 1974). N2 was the wild type (WT) strain. *C. elegans* strains were obtained from the CGC[19] unless otherwise noted.

Strains are kept on nematode growth medium (NGM) seeded with the OP50 strain of *E. coli* in circular petri dishes (Stiernagle, 2006). Organisms destined for screening or whole genome sequencing (WGS) were propagated on larger diameter plates coated with HB101 *E. coli* to facilitate larger populations.

Working strains used for this thesis were kept at 20ºC unless otherwise noted. Before using a strain for experimentation, it was maintained in a well-fed and 'clean' state for at least two generations. Cleaning from contamination was accomplished through picking worms to new plates or when needed ''bleaching'' with a fresh solution of standard bleach:1 M NaOH (1:1).

Genetic Crosses and Strains

Heat shock (HS), 45 minutes to one hour at 37º, was used perferentially in this thesis to produce males. Detailed crossing plans for special cases[20] can be found in the **Crossing Schemes** section of the Appendix. Crosses were conducted at 20º. A generalized srossing scheme is depicted in **Figure 11.** A feature of *trp-4(d)* mutants is the inability of males to produce progeny; the cause for this has not been determined so it cannot be said whether males are infertile or are

19 funded by NIH Office of Research Infrastructure Programs (P40 OD010440)

[20] Three crossing plans: general, involving the X chromosome, and crossing on the same chromosome are diagramed.

incapable of mating. In any case, the result of this is that males must be made from

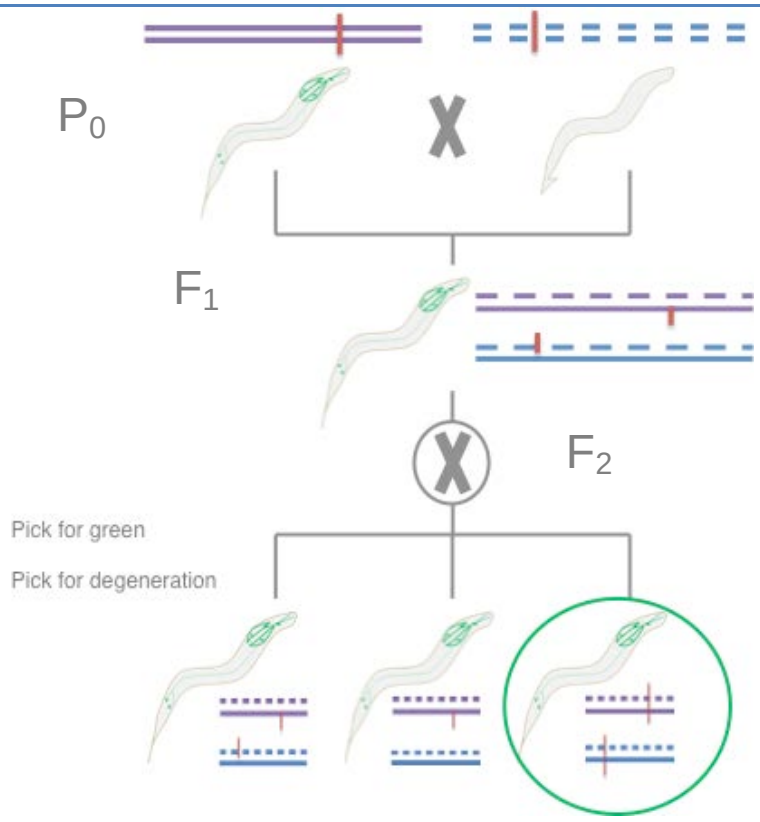

For this schematic, we assume that the Gene of Interest (GoI) is on a different chromosome than *trp-4*..

GoI strain males are produced through HS to yield homozygous GoI(*/*)

Seven hermaphrodites and fifteen males (or a similar ratio, always favoring males) are placed onto empty plates and given food. P_0 generation.

Hermaphrodites are singled from the first filial generation (F_1).

The success of the cross can be determined by observing the F1 generation. If there is an abundance of males then the cross worked.

In the F_2 generation thirty hermaphrodites are singled from a cross-progeny plate. The singled F2s are selected for degeneration, fluorescence, and for GoI phenotype (if any).

In F3 generation, the picked strains are confirmed with genotyping. Once the target strain is achieved, the experimenter will score the severity of degeneration.

Figure 11 Generalized Crossing Scheme for trp-4 (ot337) and an arbitrary gene of interest. In this scheme, a trp-4(ot337) is the hermaphrodite used in the parental cross. For chromosomes: purple indicates LG1, blue indicates LG[random], straight lines from the hermaphrodite, and dashed from the male. A circled X means self-cross. This generalized scheme is a guideline, and neglects much of genetics, including recombination. Fluorescent marker is shown with green. The target strain is outlined in the third filial generation by a green circle.

the animals mutated for the Gene of Interest (GoI) that is intended to be crossed to *trp-4(d)*. Strains built for this thesis are listed in **Table 1**. Strains were frozen with 15% glycerol solution (Stiernagle, 2006).

Table 1 Strains built for the thesis are listed in this table. Alleles are in parenthesis and LGs are bolded. vtIs1 is routinely used in this lab and its genotype (DAT-1::GFP) is often not mentioned. According to convention, genes on the same chromosome are separated by commas and genes on different chromosome are separated by semi-colons. Under the heading project, the purpose of the strain is indicated.

Strain	Genotype	Description	Experiment
MDH171	norSci1_[dat1::Trp-4(d)_unc-119]**II**;unc-119(ed3)**III**;vtIs1**V**	This is the screening strain with the ''endogenous'' copy of trp-4 crossed out.	Forward genetic screen
MDH202	trp4(ot337)**I**;vtIs1**V**;Glo-1(zu391)**X**	For scoring neurodegeneration	Lysosomal biogenesis
MDH203	trp-4(ot337)**I**;vtIs1**V;** vha-3(ok1501)**IV**	For scoring neurodegeneration	Involvement of V-ATPase
MDH240	trp4(ot337)**I**;vtIs1**V**;Vha-12(n2915sd)**X**	For scoring neurodegeneration	Involvement of V-ATPase
MDH241	zdIs5(mec-4::GFP)**I**;mec-4 (u231)**X**	Developed as control for suppression experiments	Control
MDH249	trp4(ot337)**I**;vtIs1**V**;Unc-32 (e189)**III**	For scoring neurodegeneration	Involvement of V-ATPase
MDH250	Unc-32(e189)**III**;vtIs1**V**; him-8(e1429)**IV**	Obtained from cross of MDH285	Involvement of V-ATPase
MDH251	Unc-32 (e189)**III**;vtIs1**V**	Control for scoring strain MDH285	Involvement of V-ATPase
MDH285	apb-3(ok429)**I**,trp4(ot337)**I**;vtIs1**V**	For scoring neurodegeneration	Lysosomal biogenesis
MDH286	apb-3 (ok429)**I**; vtIs1**V**	Control for scoring strain MDH285	Lysosomal biogenesis

Genotyping

To confirm the genotypes of the generated strains, PCR and gel electrophoresis were used for deletion mutants, PCR and DCAPs digestion or PCR and sanger sequencing were used for point mutations, and assessment of obvious phenotypes were used in all cases to determine correct strains.

Primer Development

There were two three different kinds of primers used in this thesis: standard, nested, and DCAPS; the latter two were usually combined. Standard primers were developed in one of two ways. Primers could be developed using the Pri-

mer BLAST tool on the NCBI database or by-eye. Generally, primers developed with Primer3 software yielded more consistent results. NCBI uses the Primer3 development algorithm to find the best primers. This has many advantages, including reporting of failed primers and thus constantly updating algorithm. It also gives the molecular analysis of the primer. It incorporates its own BLAST technology, automatically analyzing the specificity of the primer (Ye et al., 2012).

All primers were analyzed by the IDT technologies OligoAnalyzer 3.1 DNA calculator. Furthermore, if primers were not analyzed for sequence homology in the NCBI BLAST algorithm, the BLAT algorithm on WormBase was utilized, written by Jim Kent[21]. This can be found on the WormBase website. It works by compiling the genome based on non-overlapping 11 bp fragments. Either BLAST or BLAT must be used to ensure primer specificity- especially when the primers are designed by eye.

DCAPs are a kind of primer that makes detection of single nucleotide polymorphisms (SNPs) possible with standard electrophoresis. The program works by comparing the sequence with the SNP and without. It then find a specific restriction site including the SNP which will allow one to differentiate the two sequences (Neff et al., 2002). A high % agarose matrix must be used (3.3-3.5%) in order to detect the shift. This method has become irreplaceable in this lab, as the *trp-4(ot337)* mutation is detectable with DCAPs primers and does not have to be sent for sequencing every time a strain is being built. Briefly: a normal PCR is run with one of the primers developed by the DCAPs program and another developed by the experimenter, the sample is digested with the specific enzyme indicated by the program, and the sample is run on a high% agarose matrix and compared relative to the controls.

All of the primers used in this thesis can be found in the **Primers** section of the **Appendix**. They are given the generic chronological formula of: [author's initials][the next number on the list][directionality 3'->5'], ie TP1F.

[21] http://www.kentinformatics.com/

PCR

PCR was conducted as standard, following the pipetting scheme and PCR program in **Figure 12**. The pipetting scheme in **A** is adapted from the recommended PCR mix in the TAQ polymerase information packet. The general program in **B** is adjusted as needed: The T_A is typically set at 2º less than the primer T_m. The elongation time is adjusted to the 1min per 1kb formula set forth in the Thermo Scientific TAQ polymerase information packet. Heterozygous PCR controls were acquired by mixing half WT and half mutant controls.

Sequence Analysis

Sanger sequencing was performed by Macrogen. The samples sent were cleaned according to the protocol provided in (Werle et al., 1994). Sequences were aligned by DNAsequencer software and homozygosity was determined.

RNAi

RNAi, or RNA interference, is a knockdown method useful in C. elegans. Either by injection, soaking, or feeing, a double stranded (ds) nucleotide sequence is introduced to the worm. Upon recognition of dsRNA, the cell is cued to degrade all matching sequences, effectively knocking down the gene of interest (Ahringer, 2006). Unfortunately, this take-up is not efficient in the nervous system. (Timmons et al., 2001). In order to carry out knockdown system-wide, including

A

General Pipetting Scheme for PCR Reactions

Reagent	Amount (µL) x1 RXN
10x DreamTaq Buffer	2.5
10 mM dNTPs	0.5
Forward Primer	0.5
Reverse Primer	0.5
Template	4.0
TAQ	0.4
H_2O	16.6
Total Volume	25.0

B

General Program for PCR Reactions

Step	T (Cº)	Time
Initial Denaturing	95	3’
Denaturing	95	20’’
Annealing	57	30’’
Elongation	72	1’
Final Elongation	72	5’

Figure 12 PCR protocols A shows the pippetting scheme for a master mix. **B** shows the general temperature program for the reactions.

the nervous system, a strain sensitized to RNAi is utilized (Sieburth et al., 2005).

Effectiveness of RNAi was determined dually. First, the known phenotypes of the mutations were considered, in this case: developmental and embryogenesis defects were observed. Note the gonads of **A** and **B** in **Figure 13**. There are clear embryogenesis defects in the VHA-11 RNAi organism (**A**) compared with the organized and compact development seen in **B**. Secondly, an RNAi clone of known effect was used as a positive control indicative of the success of general RNAi experimental conditions (Nagarajan et al., 2014). Though this could not justify any positive or negative results, it could shed doubt on the scoring if the known results were not replicated. In this thesis, *trp-4(d)(ot337);eri-1;lin-15b;vtIs1I,* was used for RNAi experiments. Clones were grown with the standard HT115 strain of bacteria.

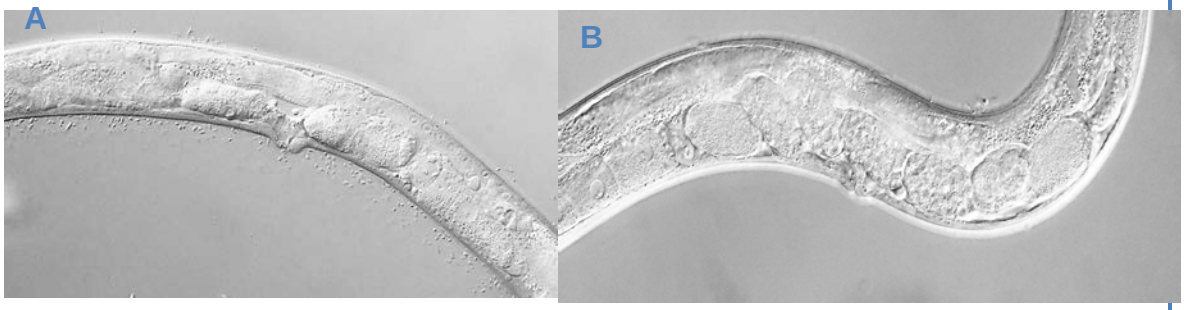

Figure 13 Effectiveness of RNAi. A and **B** both show adult animals. **A** was fed on VHA-11 RNAi **B** is a WT worm fed on OP50.

All possible *vha* (controlling the V-ATPase pump) genes were considered. Most of the genes are embryonic lethal- making experimentation at the L4 stage difficult indeed. To overcome this, the progeny of RNAi-fed L4 animals were scored. This was done so that some of the maternal development programs could be properly initiated. Survival rates were very low in all cases, and in the case of VHA-4, nothing could be done to alleviate the effects of its absence.

Pharmacological inhibition of V-ATPase pump

Bafolimycin A (50μM, Sigma) was injected into the body cavity of the worm as previously described, (Syntichaki et al., 2005), to inhibit the V-ATPase pump pharmacologically. The chemical was injected into the body cavity. The chemical was dissolved in DMSO (Sigma) and the mix was brought to concentration with nuclease free water. DMSO and nuclease free water served as the experimental control.

Microscopy

To select worms with fluorescent markers during crosses, the Zeiss Discovery.V12 stereoscope was used. Scoring dopaminergic head neurons was completed with the Zeiss imager M.2 microscope. Differential interference contrast (DIC) was integrated into this microscope and was used for scoring and visualizing morphology. Images were taken and created by the Zeiss software.

Scoring

For dopaminergic and mechanosensory degeneration: In the scoring book, cells were counted as: 1 (healthy soma and healthy dendrite), ł (soma but no dendrite), and 0 (neither a healthy soma nor dendrite). Swollen, shrunken, and rounded cells were not considered healthy. Neurons with faded nuclei were not considered healthy. Dotted or interrupted projections were not considered healthy. Absence of either was scored as 0. Worms were immobilized with 50μM sodium azide.

Development of transgenic line

To visualize the lysosomes during *trp-4(ot337)*-induced cell death, the (Lysosome associated membrane protein) LMP-1 lysosomal marker (Kostich et al., 2000) was cloned under a DAT-1 promoter (**Figure 14**), and microinjected into the *trp-4(ot337)* strain.

Cloning

LMP-1::GFP was amplified from strain *unc-119(ed3);pwIs50*. pwIs50 [lmp-1::GFP + Cbr-unc-119(+)][22] (Treusch et al., 2004). Primers TP64F and TP65R[23] were used to amplify the LMP-1::GFP fusion from this strain (**Figure 14A**); their sequences can be found in the Crossing Schemes section of the Appendix. The high fidelity Phusion enzyme (Thermo Scientific) as the resulting fragment is quite large at 1803 bp. The band was excised and gel purified according to the Quiagen Gel Extraction Kit protocol. The PCR product and vector were cut with Thermo Scientific enzymes KpnI and EcoRI in a double digest. In the vector, the enzymes cut out GFP (**Figure 14B**). Ligation and transformation were performed as standard; DH5α was used as competent bacteria for transformation. Colonies grew in both V+H_2O and V+I plates, with more on the later. Colonies were subjected to a colony PCR (**Figure 14C**). The colonies with V+H_2O did not show any band, meaning the vector did not take up insert. Three colonies V+I showed a positive PCR result. Two of these were chosen for a culture PCR, along with one of the V+H_2O colonies. Curiously, all three colonies showed positive for LMP-1::GFP, indicating that the V+H_2O sample was contaminated at some point (**Figure 14D**). the colonies were sequenced with three different primers annealing to the pDAT-1 sequence, outside GFP, and within GFP. LMP-1::GFP was successfully cloned into the pPD95.75 plasmid (**Figure 14E**) (AddGene) with DAT-1 promoter (**Figure 14F**). There was an alternative strategy involving cloning LMP-1 in between dat-1 and GFP in the pPd95.75 vector. However, no colonies grew.

[22] Ordered from CGC.
[23] Note that TP65R will not anneal in a WT worm, as it anneals to the COOH terminus of GFP.

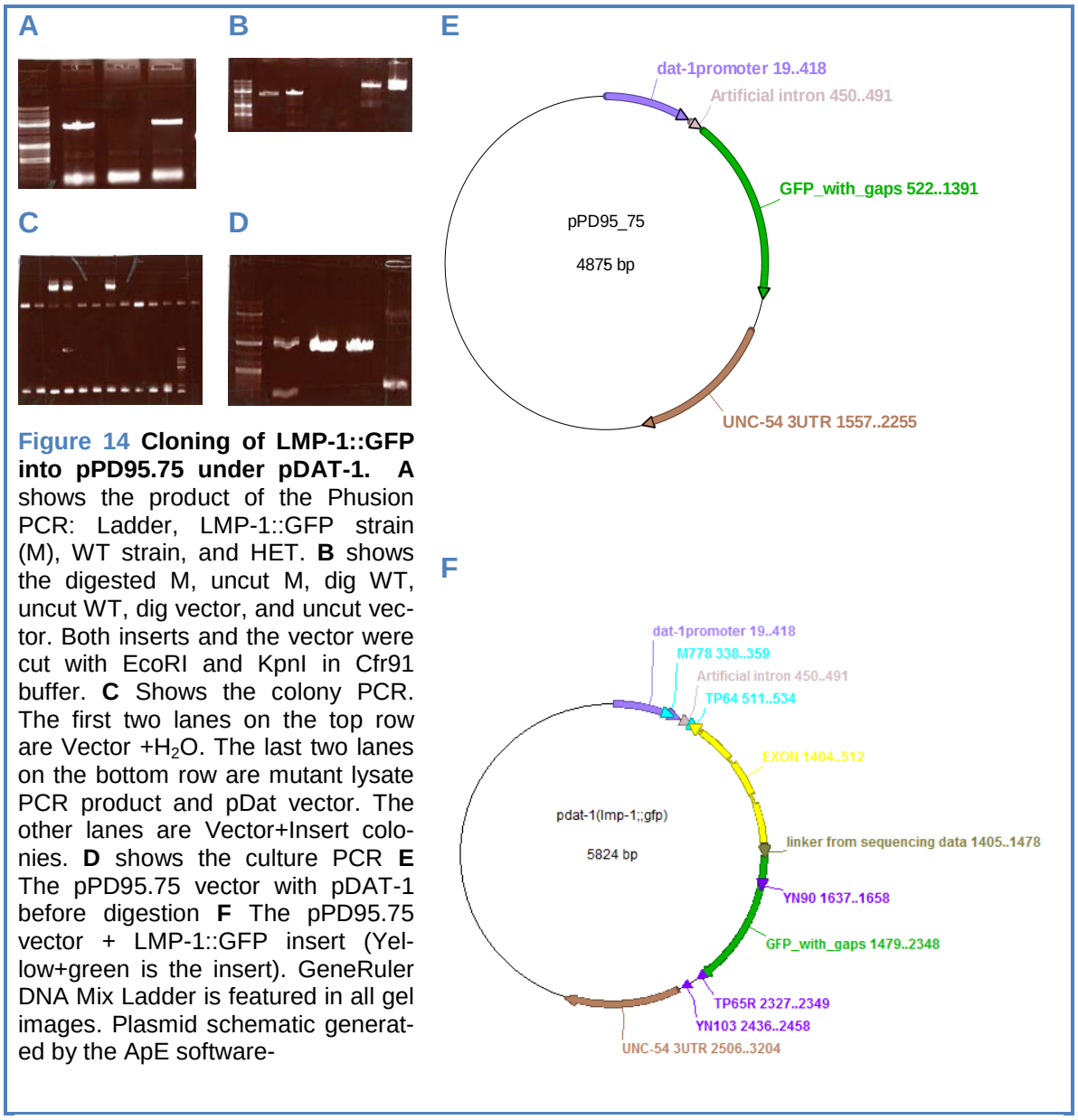

Figure 14 Cloning of LMP-1::GFP into pPD95.75 under pDAT-1. **A** shows the product of the Phusion PCR: Ladder, LMP-1::GFP strain (M), WT strain, and HET. **B** shows the digested M, uncut M, dig WT, uncut WT, dig vector, and uncut vector. Both inserts and the vector were cut with EcoRI and KpnI in Cfr91 buffer. **C** Shows the colony PCR. The first two lanes on the top row are Vector +H_2O. The last two lanes on the bottom row are mutant lysate PCR product and pDat vector. The other lanes are Vector+Insert colonies. **D** shows the culture PCR **E** The pPD95.75 vector with pDAT-1 before digestion **F** The pPD95.75 vector + LMP-1::GFP insert (Yellow+green is the insert). GeneRuler DNA Mix Ladder is featured in all gel images. Plasmid schematic generated by the ApE software-

Microinjection

To realize the cloned plasmid *in vivo*, it must be introduced into the genome of *C. elegans*. The injected plasmids were introduced extrachromosomally. The technique of microinjection utilized is thoroughly described in the *C. elegans Microinjection Protocol* written by Catarina Silva of Northwestern University. The microinjection mix was made with the newly obtained plasmid[24] from the LMP-1::GFP cloning and selected coinjection markers (roller for easy picking and PBS for weight) with a total ideal mass of 150ng (**Table 2**). A dark *trp-4(ot337)* strain was used for injection, as the transgene had a GFP in it. Young adults were used for injection. The animals were picked to an empty plate and left to roam for an hour. This mildly starves the worm, but it also allows the animal to defecate which makes visualization of the gonad easier. The animals were picked to a dehydrated 2% agarose pad into a drop of injection oil. After injection, the worm was gently moved to a fresh plate full of food and rehydrated with 9 µL of M9 buffer. A Leica inverted DIC microscope with a movable stage was used to view the worms during injection. An Eppendorf FemtoJet express was used as the injection device. Pre-made injection needles were purchased from Eppendorf.

Table 2 Extrachromosomal lines generated during the thesis are listed in this table. *trp-4(*ot337), notably without any reporter, was used as the starting strain for the injection.

Strain	Genotype	Description
MDH242	norEx86[Pdat-1::lmp-1::gfp;rol-6];trp-4(ot337)	Lmp-1 injected at 10 ng/ul, 40 ng/ul rol-6, and 80 ng/ul PBS into strain *trp-4(ot337).*
MDH296	norEx86[Pdat-1::lmp-1::gfp;rol-6]	generated by crossing out *trp-4(ot337)* from strain

Preconditioning

The HS preconditioning experiment was performed as previously described (Kourtis et al., 2012). Breifly: adult animals, *zdIs5;mec-4(u231)* and *trp-4(ot337);vtIs1*, were bleached and the eggs centrifuged and washed with M9 buffer. Eggs were suspended in M9 and subjected to a water bath treatment, one

[24] Quiagen DNA purification kit was used for plasmid purification.

group of each genotype at 20ºC and one at 34ºC, for twenty-five minutes. All four groups were transferred to agar plates with NGM (Kourtis et al., 2012). In deviation from the protocol: after bleaching and washing, eggs were kept nutating at RT for four to five hours. This step was altered to ensure that embryos would have a gentle environment to hatch after the stressful heat shock treatment.

Forward genetic Screen

The forward genetic screen was conducted in accordance with the protocol described in (Doitsidou et al., 2008) (**Figure 15A**). EMS was used as the mutagen. The COPAS BioSort worm sorter was used to automatically screen mutants. Three rounds of screening were completed by the author (**Table 3**). Confirmed mutants can be found in the Results and Discussion section.

Table 3 **Screening Rounds** Screening strain '530' is *norSci1_ [dat1::Trp-4(d) _ unc-119] II; unc-119(ed3)III; trp-4(ot337)I;vtIs1*

Screen round	Strain	Mutagenesis date	#P0s mutagenized	#F1 plated	#F2s screened
NorMut1	530	05.08.2013	2650	2750	~1000
NorMut2	530	15.08.2013	11910	45000	50400
NorMut3	530	16.09.2013	6267	54900 eggs	TBD

The screening strain was *norSci1_ [dat1::Trp-4(d) _ unc-119] II; unc-119(ed3)III; trp-4(ot337)I;vtIs1.* This strain has two copies of the mutated channel: one on chromosome I (endogenous) and one on chromosome II (Mosci inserted). Additionally, another strain was created in which the endogenous copy was absent. Thus, there were three relevant combinations: the original strain with one copy of the mutated channel on chromosome I, a strain with a copy of the mutated chan nel on chromosome II, and a strain with two copies of the mutated channel- one each on chromosome I and II. The three are compared for levels of degeneration in **Figure 16**. It seems, as previously suspected by Nagarajan et al, that degeneration is dependent on dosage of the mutated *trp-4(d)* gene.

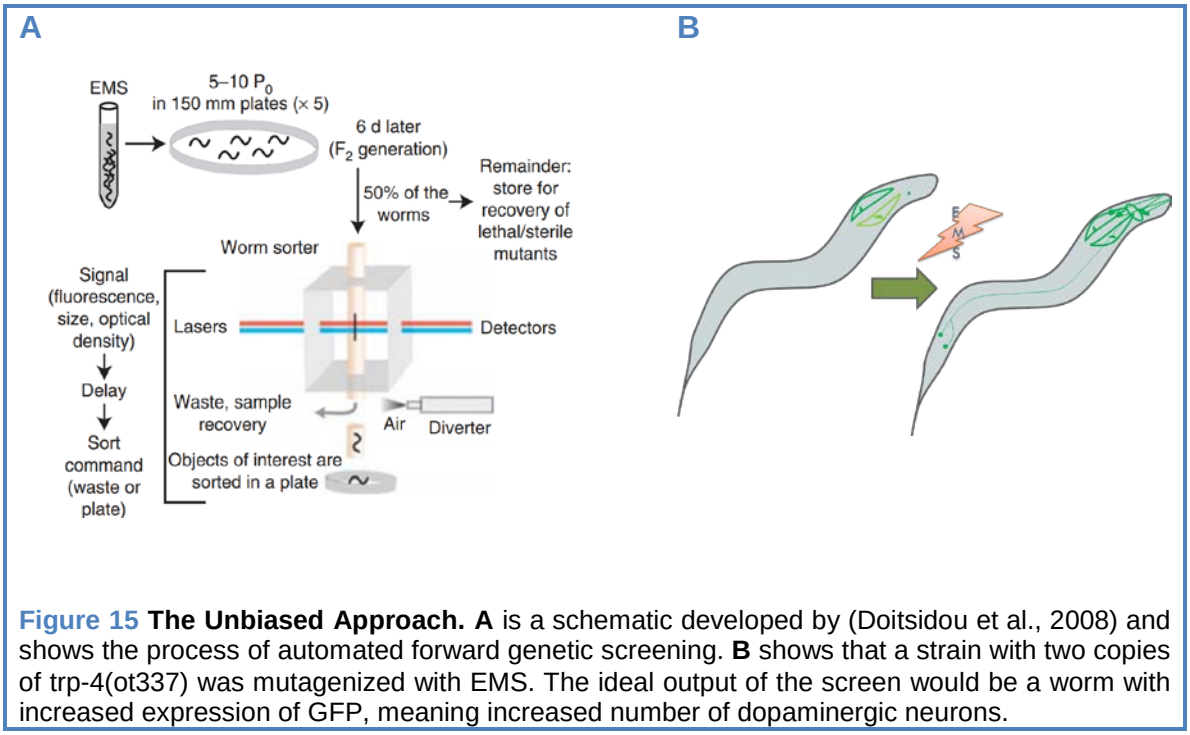

Figure 15 The Unbiased Approach. A is a schematic developed by (Doitsidou et al., 2008) and shows the process of automated forward genetic screening. **B** shows that a strain with two copies of trp-4(ot337) was mutagenized with EMS. The ideal output of the screen would be a worm with increased expression of GFP, meaning increased number of dopaminergic neurons.

Suppressor selection was automated by selecting for the highest levels of GFP (**Figure 15B**). Isolated candidate suppressor mutants were confirmed for their partial or full suppression of degeneration. Suspected partial mutants were confirmed by scoring against *trp-4(ot337);vtIs1*. This strain was chosen over the screening strain because it had more head neurons than either of the other two strains. Thus, if a strain was found to be significantly better than it, it could be considered a true suppressor. Suspected full suppressors were confirmed to be intergenic by crossing to a wild type strain (*otIs356[rab-3::NLS::tagRFP]V;him-8(e1489)IV)*. The F_1 generation was observed for degeneration. If it was ob served, the mutant was a recessive full suppressor and if none was observed, ten to twenty individuals were singled. If their progeny did not exhibit degeneration, the mutation was deemed intragenic, if it did, it was declared a dominant suppressor.

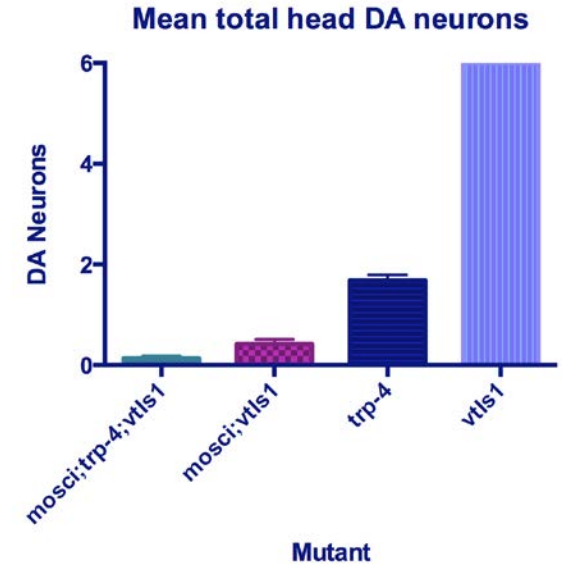

Figure 16 Comparison of strains with trp-4(d). ''Mosci'' refers to the copy of trp-4(d) that was inserted using the Mosci method.

WGS sequencing was provided by BGI Tech Solutions (Hong Kong). The genomic samples sent were cleaned according to the protocol provided with the DNeasy Blood and Tissue kit. Samples were left to rest in the elution buffer >24 hours after precipitation because they did not dissolve following the standard protocol and time.

Statistics

Normalcy of the population was determined by plotting the values for average head neurons per worm of a population of *trp-4(ot337)* group of animals on a frequency histogram, **Figure 17**. The distribution is close to Gaussian, and thus parametric testing is appropriate. Additionally, the D'Agostino & Pearson omnibus normality test found the population to be consistent with Gaussian assumptions in the Prism6 (GraphPad) software.

After scoring, values for degeneration were entered into Excel 2010 (Microsoft). '1' was entered if the soma and dendrite were present and '0' if either was missing. After all values were entered, each dopaminergic class was individually summed and divided by the number of individuals scored. Individual values ranged between 45 and 55, though the ideal value was 50. The standard error of the means (SEM) was calculated within Excel by dividing the standard deviation of the values by the square root of individuals scored. Statistical analysis was continued in a separate software.

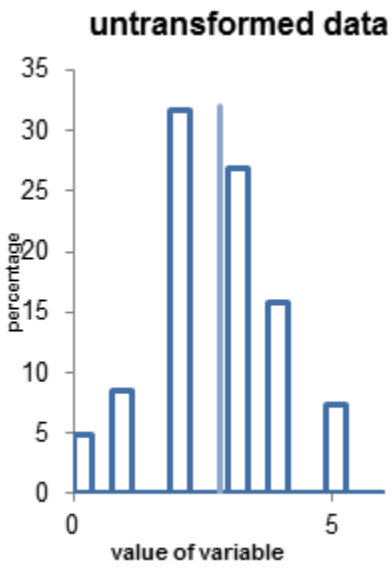

Figure 17 Distribution of trp-4(d) degeneration is shown here in a frequency histogram. The histogram was created by Dr. John MacDonald of the University of Delaware. The graph shows the distribution of the total head neurons (min=0, max=6) for a population of trp-4(ot337) animals (n=82).

All statistics and graphs were generated by the Prism6 software (GraphPad). For calculations of separate dopaminergic classes, two-way ANOVA was performed. For comparisons of total head neurons, one-way ANOVA statistical regression was performed and the unpaired t-test with Welch's correction (As the means had variance in the SD.). Multiple comparisons were achieved using Sidak's post hoc analysis. Significance was attained when $p<0.05$. Significance assignments in Prism6 software: *=0.05, **=0.005, ***=0.0005, and ****=0.00005.

Literature Search

The starting place for the literature search was papers used during the experimental procedures. Beyond the methods of these papers were introductions and discussions containing references of previous experimentation. These sources were read and also scoured for further sources relevant to the field.

Google Scholar in particular was a useful search engine for this thesis. The search algorithm used also included the UiS proxy for access to publications. Thus, no searching for papers through the university systems was required. Many of the Google Scholar links used NCBI's PubMed database.

The UiS database was connected to remotely when not at a UiS computer with the Bibsys[25] network, which connects all of the Norwegian libraries and their access rights. UiS utilizes the Oria search system, provided by Bibsys.

EndNoteX7 was used to compile the references. ReadCube was used to organize, read, and notate relevant PDF documents.

[25] Accessed remoted with the URL: http://www.uis.no.ezproxy.uis.no/

Results & Discussion

Candidate approach

Effect of V-ATPase lysosomal acidification

trp-4(d)[26] mutants exhibit severe and progressive degeneration in their dopaminergic neurons. In order to assess whether the function of V-ATPase (vacuolar H^+ ATPase) pump is important for the dopaminergic cell death induced by *trp-4(d),* both genetic and pharmacological methods were employed. The V-ATPase pump has two sectors based on their location on the lysosomal membrane: the V_0 sector of the pump is cytoplasmically located, while the V_1 sector is membrane-bound. Subunits from both sectors were tested by crosses and RNAi. Various V-ATPase subunits were prioritized for testing based on the following criteria:

- Reported expression in the nervous system
- Previous implication in necrotic cell death in mechanosensory neurons (Syntichaki et al., 2005)
- Availability of mutants/ RNAi clones

A summary of the *vha* genes can be found in **Table 4**.

Genetic Approach

VHA-12 is responsible for encoding a major subunit of the V_0 sector. It is required for embryogenesis as well as morphogenesis; v*ha-12* null mutations are lethal. In a screen for jerky locomotion, the Jorgensen lab isolated a viable semi-dominant allele in the *vha-12* locus, *n2915sd*[27]. This allele is a substitution of a highly conserved amino acid position, A385, that likely results in impaired ATP catalysis (Ernstrom et al., 2012). It was previously shown to suppress *mec-4(d)* degenera

[26] *trp-4(ot337)* is used interchangeably with *trp-4(d)*.
[27] Kindly provided by the Jorgensen lab at the University of Utah.

Table 4 V-ATPase pump genes and their expression patterns and mutant phenotypes. In column one, an asterisk indicates known neuronal expression. All genes tested in mec-4(d) gave suppression. This table is adapted from Table S1 in (Syntichaki et al., 2005)

Gene	Sector, Subunit	Allele/RNAi	Effect in mec-4(d)	Comments and Outcomes
vha-1	V_0, c-subunit	RNAi	n/a	lethal
vha-2*	V_0, c-subunit	n/a	yes	RNAi sequence not correct
vha-3	V_0, c-subunit	ok1501	n/a	mild effect
vha-4	V_0, c''-subunit	RNAi	n/a	lethal
vha-5	V_0, a-subunit	n/a	n/a	RNAi not available
vha-6	V_0, a-subunit	RNAi	n/a	no effect
vha-7	V_0, a-subunit	ok1952	n/a	cross could not be completed
vha-8	V_1, E-subunit	n/a	n/a	RNAi available, not completed
vha-9	V_1, F-subunit	n/a	n/a	RNAi available, not completed
vha-10*	V_1, G-subunit	RNAi	yes	no effect
vha-11	V_1, C-subunit	RNAi	no	inconclusive
vha-12*	V_1, B-subunit	n2915sd	yes	mild effect
vha-13	V_1, A-subunit	n/a	n/a	RNAi sequence not correct
vha-14	V_1, D-subunit	n/a	n/a	RNAi sequence not correct
vha-15	V_1, H-subunit	n/a	n/a	RNAi available, not completed
vha-16	V_0, d-subunit	n/a	n/a	RNAi not available
vha-17	V_0, e-subunit	RNAi	n/a	inconclusive
vha-18	V_1, H-subunit	n/a	n/a	RNAi available, not completed
vha-19	V_0, AC45-subunit	n/a	n/a	RNAi available, not completed
spe-5	V_1, B-subunit	hc93	yes	not completed for thesis
unc-32	V_0, a-subunit	e189	yes	no effect

tion (Syntichaki et al., 2005). A double mutant of *vha-12(n2915sd)* and *trp-4(ot337),* with *vtIs1[dat-1::GFP]* in the background, was created to see if the VHA-12 protein has an involvement in *trp-4(d)* induced degeneration. L4 animals of this strain were scored against *trp-4(ot337);vtIs1* and *vtIs1* itself (omitted from the graphs) (**Figure 18**). **Figure 18A** shows that significant differences were observed between the strains when scoring individual classes of head neurons (CEPV, CEPD, and ADE), but no such difference when comparing the total head neuron counts. While the CEPs showed a small but significant protection from

degeneration in the *vha-12* mutant, the ADEs seem to be trending in the opposite direction towards more degeneration. Thus, when analyzing all head neurons together, any protection gained in CEPs is negated by the ADE value, resulting in a non-significant effect for total DA head neurons.

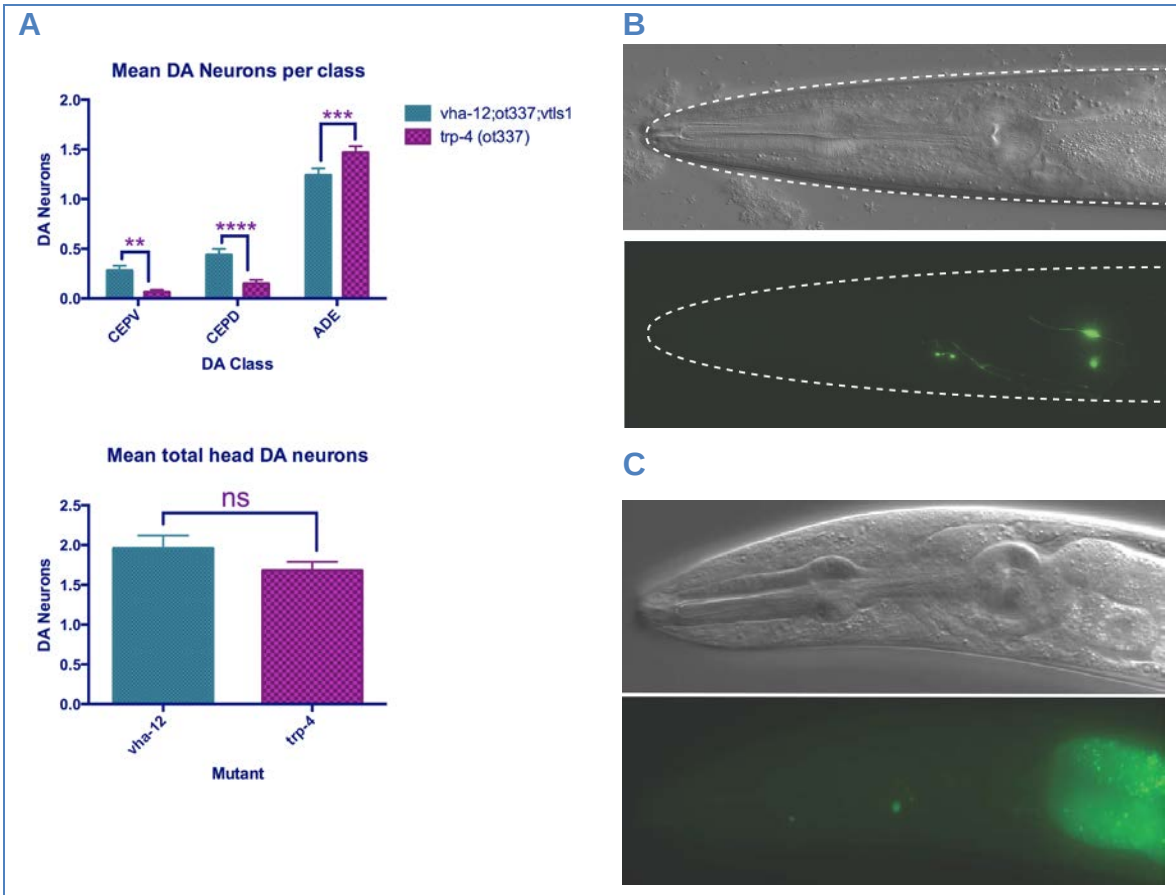

Figure 18 Effect of vha-12 (n2915sd) mutation in trp-4 (ot337) animals. Graphs in **A** show the mean DA neurons per class on top, and the mean total head DA neurons on the bottom. Non-significant values are indicated by 'ns.' All significant values are indicated by *. Calculations were done with SEM. Multiple comparisons within the graphs were determined with Tukey's test. Alpha was 0.05. Two-way ANOVA for the top graph and one-way ANOVA with the bottom graphs. The control strain vtIs1 (DA head neurons per worm=6, per category=2) was significant in all comparisons, but is omitted from these graphs. For *vha-12* mutant, n=50 and *trp-4(d)* n=47. **B** shows a *trp-4(d)* worm **C** shows a *vha-12;trp-4* double mutant. In both B and C, only ADE neurons are still present (compare to wild type on page XXX of this thesis). For both images, objective magnification is 40x, DIC on top and GFP MIP (maximum intensity projection) below. All figures generated from L4 animal data. Image credit, *trp-4(d)* worm: Dr. Doitsidou.

Nonetheless, when considering CEPs versus ADEs it is conceivable that the different DA classes may vary in their susceptibility to protection as much as they

vary in their susceptibility to degeneration; with CEPs being more susceptible on both counts in comparison to ADEs- in this case. Of course, we also cannot rule out the possibility that there exist scoring errors. As with all of the results generated in this thesis, scorings will need to be performed at least three times, in a blinded way, with n>50 each time to confirm a suspected effect.

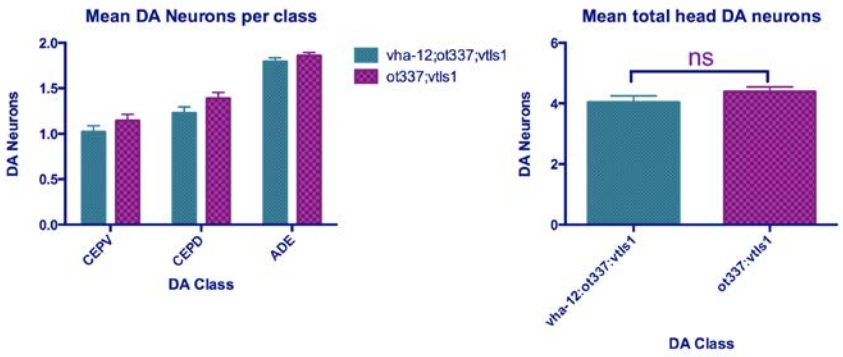

Figure 19 L1 animals of *vha-12(n2915sd)* and *trp-4 (ot337)* double mutant did not experience any of the protection seen in L4 animals. No results were significant, except those with the control vtIs1 (****).

trp-4(d) degeneration begins at an early developmental stage. To determine if the observed mild protection conferred by the *vha-12* mutation in CEPs in adult animals could be more pronounced in early stages, the scoring was repeated with L1 animals, **Figure 19**. No suppression was seen in L1 stage. It seems that the effects of *vha-12* might be dependent on developmental stage. Scoring should be repeated for L1 *through* L4 to confirm the observed trends.

Additionally, one could look at one through five-day-old adults and see if the mild protective effect in CEPs holds with advanced aging. Additional alleles of this gene could be tested for their effect on dopaminergic degeneration. However, as Ernstrom et al. reported, while the *n2915sd* allele is the weakest of the described *vha-12* alleles, it is also viable. Finally, this strain was not scored blindly in the L4s, but was in the L1s. A 'blinded' experiment gives more reliable results than an experiment where we are aware of the genotypes under investigation.

Further V-ATPase subunits were tested for involvement in *trp-4(d)* induced degeneration; genetically in **Figure 20** and with RNAi treatment in **Figure 21.** *vha-3*, *unc-32*, and *vha-7* were chosen as genetic candidates to test. Figure 20**A** shows the results of the *unc-32(e189)* cross. *e189* is a G to A transition and results in a partial loss-of-function mutation (Pujol et al., 2001). There was no significant difference between any of the means, except with the control vtIs1 (not shown). **Figure 20B** shows the effects of a *vha-3(ok1501)* allele on *trp-4(d)* degeneration. o*k1501* is an allele from the *C. elegans* Gene Knockout Consortium. It results in a complex substitution of a 710 bp sequence with a 2 bp sequence that causes a frameshift. There was no effect in the CEPs with this mutant and also no effect on total head neurons. However, there was a protective effect in

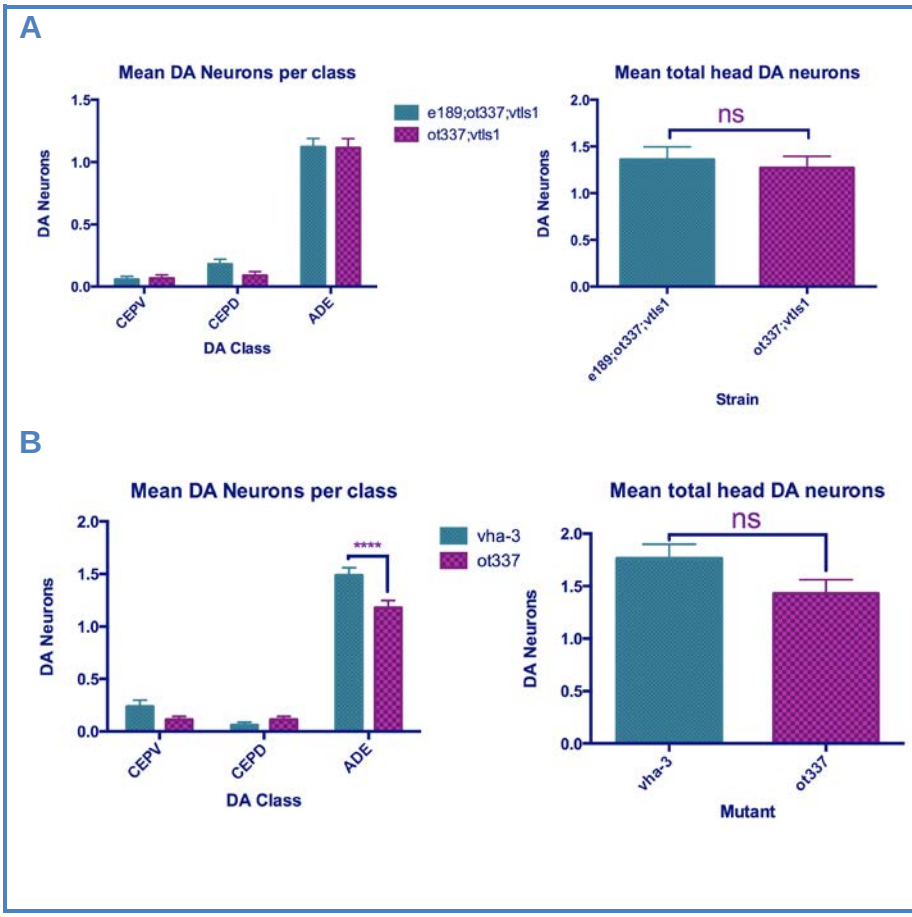

Figure 20

V-ATPase subunits further tested for effects on trp-4(ot337) degeneration. A shows the scoring results for the unc-32(e189) and trp-4(ot337) double mutant. UNC-32 encodes the a-subunit in the V0 Sector (membrane bound) of the V-ATPase pump on the lysosome. *e189* n=50, *trp-4* n=44 **B** shows the results for the vha-3(ok1501) and trp-4(ot337) double mutant. VHA-3 encodes for the c subunit in the V0 sector. All mutants were significantly different than the control vtIs1.

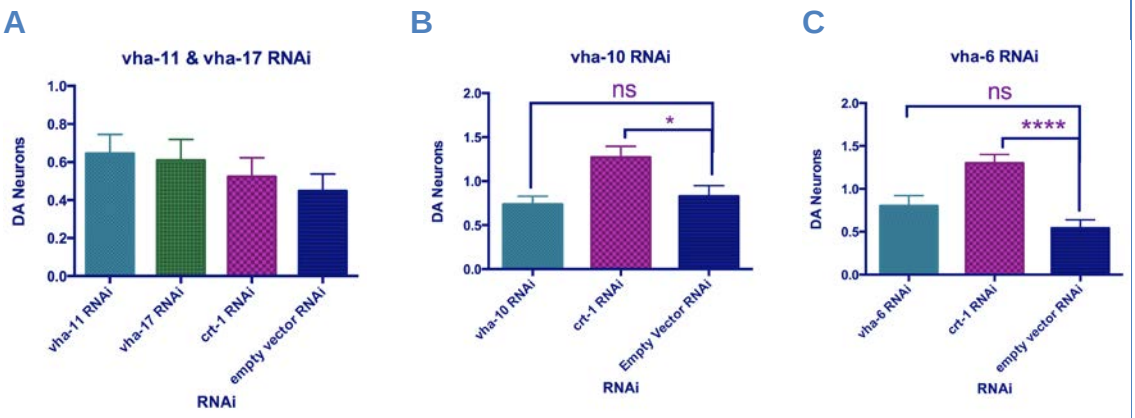

Figure 21 RNA Interference on V-ATPase Pump Subunits Subunits in both the **A** and **C** V_1 (A, VHA-11 and C, VHA-10) and **A** and **B** V_0 (A, VHA-17 and B, VHA-6) sectors were tested. In B and C, both VHA RNAi treatments were worse than CRT-1 treatment and ns with empty vector, so the DA class graph is not shown. **A** *vha-11* n=45, *vha-17* n=41, *crt-1* n=44, and *empty vector* n=49 **B** *vha-10* n=53, *crt-1* n=48, and *empty vector* n=41 **C** *vha-6* n=50, *crt-1* n=50, and *empty vector* n=48.

the ADE DA class. Crossing of *vha-7* mutants was unsuccessful because of low mating efficiency and a lack of male availability, so this mutant could not be tested.

Since there was a protective trend in the *vha-3* mutant with ADEs, and a protective trend in CEPs in the *vha-12* mutant, it would be interesting to see if a double mutant between *vha-12* and *vha-3* would show a stronger or even synergistic effect.

VHA-6, VHA-10, VHA-11, and VHA-17 were additionally tested through RNAi, **Figure 21**. In **Figure 21A** the VHA-17 and VHA-11 RNAi treatments are shown along with control RNAi treatments CRT-1 (which was previously shown with mutants and RNAi to suppress *trp-4(d)* degeneration (Nagarajan et al., 2014)) and empty vector. Though there seems to be suppression with VHA-11 and VHA-17, it cannot be determined if this effect implies involvement. This round of treatments did not pass its controls; the positive control, CRT-1 RNAi, normally suppresses *trp-4(d)* degeneration in dopaminergic neurons and was not significantly different from empty vector in this case. This can be due to many variables, including, but not limited to: plate freshness, IPTG quality, and a clean culture of

each RNAi clone. This experiment will need to be repeated to see if the protection with can be reproduced. The VHA-4 RNAi proved to be lethal and could not be overcome by performing RNAi on L4 (instead of younger) worms and scoring their progeny. **Figure 21B** and **C** show the VHA-10 and VHA-6 RNAi treatments. The controls for both were passed. In both cases, *crt-1* RNAi treatment partially suppressed degeneration. However, none of the two were different from the empty vector.

Only three of the V-ATPase pump genes have reported expression patterns in neurons (*vha-12*, *vha-10*, and *vha-2*), but one of the genes for which we observed a protective trend, *vha-3*, does not. In choosing genes to test, we did not exclude genes solely on the basis of their lack of reported expression in the nervous system as reported expression pattern can be incomplete.

Pharmacological Approach

Although in previous studies on the *mec-4(d)* model of degeneration it was possible to observe protective effects through single-gene knockdowns, it is not clear to what degree the genes coding for the V-ATPase pump subunits are redundant. Thus, eliminating or compromising one of the factors genetically may not block the function of pump. In contrast, chemical inhibition bypasses redundancy issues and thus can be more effective. We used the chemical bafilomycin, which

inhibits the pump. With this chemical, acidification of the lysosome is compro-

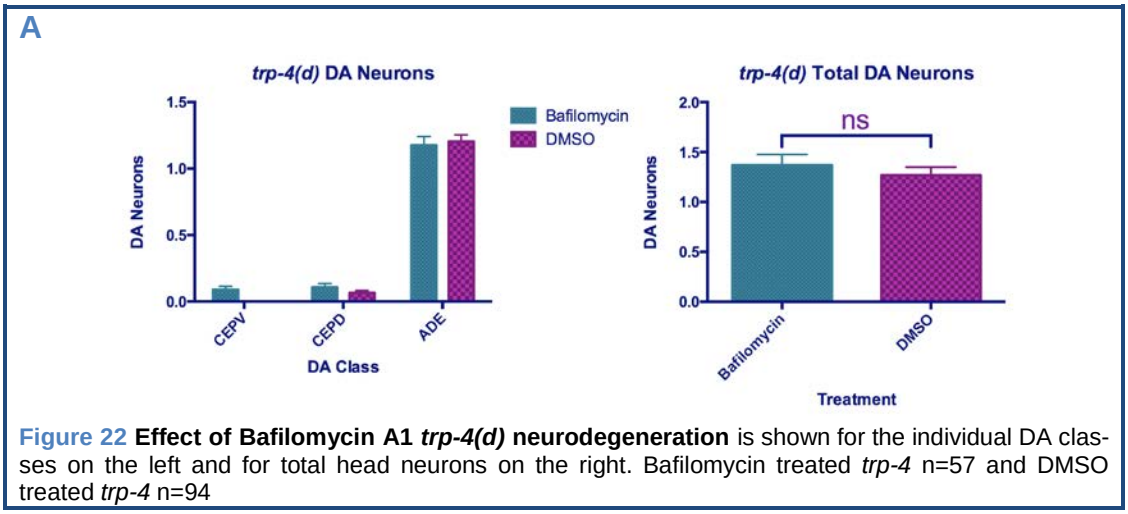

Figure 22 Effect of Bafilomycin A1 *trp-4(d)* neurodegeneration is shown for the individual DA classes on the left and for total head neurons on the right. Bafilomycin treated *trp-4* n=57 and DMSO treated *trp-4* n=94

mised and degradation of lysosomal contents does not properly occur; both consequences of V-ATPAse pump inhibition by bafilomycin (Yoshimori 1991). Bafilomycin A1 (50 µM, Sigma) was injected into the body cavity of gravid hermaphrodites (Syntichaki et al., 2005), and DMSO with nuclease-free water was injected into control animals. Progeny of injected hermaphrodites were scored at L4 stage. **Figure 22A** shows the results of the scoring. There was no significant effect with this treatment.

In order to determine if the lack of effect meant a lack of involvement of the pump- or rather a failure in delivery of the chemical- *mec-4::GFP;mec-4(u231)* animals were similarly injected as a positive control. Due to low numbers of the population scored, the control was not conclusive to determine if the treatment was effective or not.

Injecting the chemical directly in the body cavity was previously used to successfully inhibit the pump in the *mec-4(d)* model. It seems that the bafilomycin chemical is capable of penetrating across gonadal tissue. In order to have any effect on the embryos, it must also be capable of penetrating the eggshell as well as the embryonic sheath at later stages (Altun, 2009). Alternatively, one could soak the embryos in the chemical, though the chemical is harmful and thus this would need to undergo a concentration range to determine the best concentration and time at which to perform the experiment. Finally, it is necessary to perform the method in a way as to reproduce previous results in the *mec-4(d)* model. When optimization has been performed and the method is capable of reproducing past result- then reliable results can be produced for this experiment and conclusions regarding the V-ATPase pump can be drawn.

Previous experiments explored the roles of calpain and aspartyl proteases in the *trp-4(d)* model (Bachelor's Thesis, Maugard, 2013). Unlike results with the *mec-4(d)* channel, genetic manipulation of these factors did not yield significant neuroprotective or cytotoxic effects. Both pathways, the activation of proteases and the V-ATPase pump, are thought to be involved in lysosomal acidification and rupture. As such, both have been shown to be effectors of necrotic cell death

suppression (Syntichaki et al., 2002) (Syntichaki et al., 2005). Even if these factors indeed play a role in *trp-4(d)* mediated degeneration, it is possible that the hyperactivated *Trp-4(d)* channel is too cytotoxic or acts too acutely for mild protection to be discernable. Yet, it was shown previously that it is possible to significantly suppress dopaminergic degeneration in the *trp-4(d)* model, for example with intracellular Ca^{++} manipulations (Nagarajan et al., 2014). Thus, there exist pathways through which one can interfere with such acute neuronal insult. It remains to be seen if lysosomal acidification is one of these pathways, and to what degree it is involved in *trp-4(d)* cell death. To this end, the question of redundancy needs to be addressed; both the proteases and the pump genes have been explored, but have been done so with single-gene-knockdowns. Double mutants or double RNAi treatments could be the key for potent protection of dopaminergic neurons.

Lysosomal biogenesis

Artal-Sanz et al. showed that mutations in the lysosomal biogenesis pathway led to suppression of m*ec-4(d)* induced degeneration; the group found that mutations impairing lysosomal biogenesis suppressed death whereas those that increased biogenesis increased death. To test if lysosomal biogenesis is involved in *trp-4(d)* induced degeneration, the *glo-1(zu391)* gene was crossed with the trp-4 mutant, **Figure 23**. One allele of the *glo-1* gene (*zu391*) was tested in this thesis (**Figure 23A**) and was found to partially suppress *trp-4(d)* degeneration throughout all DA classes and had a significant effect when all head neurons were considered. The protective effect provided by the *glo-1* mutant is not complete **Figure 23D** when compared to *trp-4(d)* **Figure 23C**, but significant.

Expression patterns have localized GLO-1 to the gut (Hermann et al., 2005). Yet, it seems to have an effect in the DA system. There are two main possibilities here. The first is that *glo-1* is expressed in dopamine neurons. Alternatively, if GLO-1 is indeed gut-specific, then it is possible that there is a cell non-autonomous effect. This can be tested by tissue-specific rescue experiments.

Finally, it will be necessary to test more *glo-1* alleles, and additional lysosomal biogenesis pathway mutants, for example the other *glo* genes.

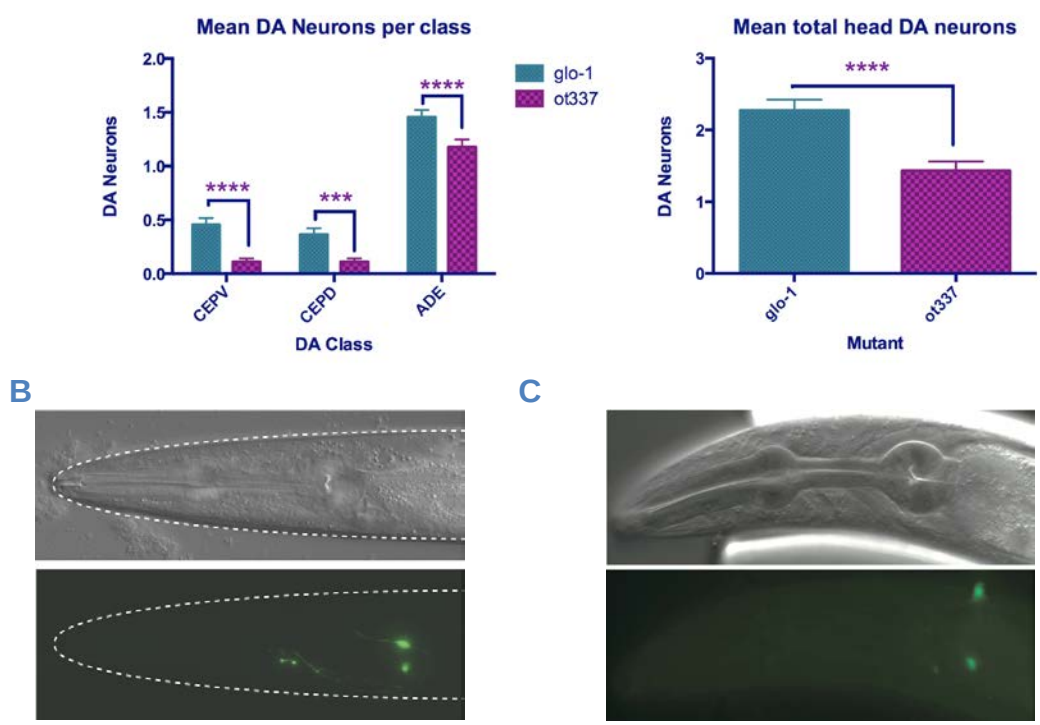

Figure 23 Effect of Lysosomal Biogenesis on *trp-4(ot337)* degeneration. Scoring data for allele involved in lysosomal biogenesis seen in **A** (*glo-1* n=44, *trp-4* n=51) The *trp-4(d)* mutant is seen in B, and the double mutant with *glo-1(zu391)* is seen in **C.** *trp-4(d)* image credit to Maria Doitsidou.

Lysosomal Reporter

The lysosomes in the *mec-4(d)* model exhibited perinuclear clustering as well as enlargement and ultimately loss of lysosomes, most likely through rupture (Artal-Sanz et al., 2006). To determine if these events also transpired in the *trp-4(d)* model, a lysosomal reporter needed to be generated in the DA neurons. To this end, the commonly used LMP-1::GFP reporter was expressed under a DAT-1 promoter, **Figure 24**. Lysosomes are clearly and specifically marked by this reporter and one can even observe dynamic transport events happening in real time. When the neuronal projections are observed, marked vesicles can be seen in the axons.

A

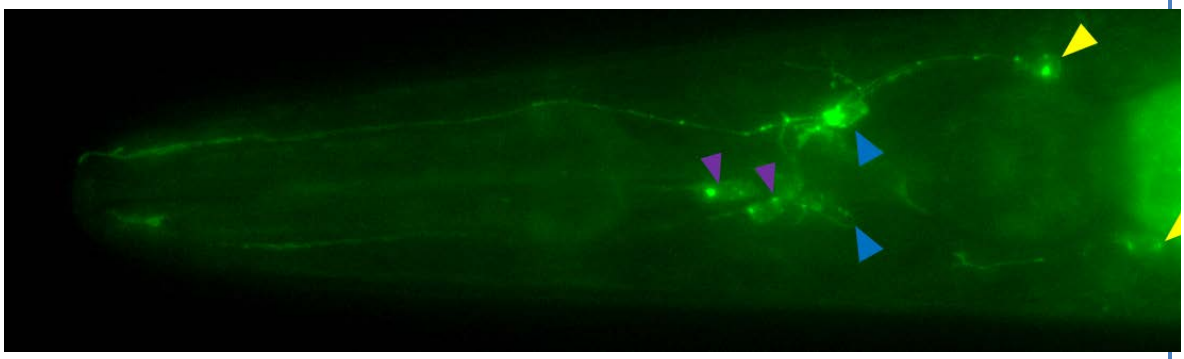

B

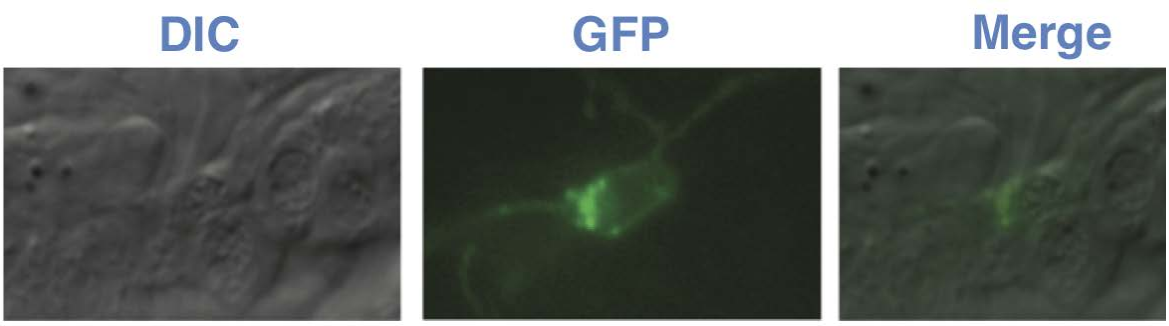

Figure 24 LMP-1::GFP under a DAT-1 Promoter. In **A**, the different DA classes are marked by colored arrows. From anterior to posterior: CEPVs: purple, CEPDs: blue, and ADEs: yellow. Image was taken at 40x objective. **B** shows a panel of left to right: DIC, GFP, and a merged image at 30% transparency. Image taken at 100x objective.

This reporter was crossed into the *trp-4(d)* mutant **Figure 25**. Lysosomal morphology was observed for differences with the wild type. In **Figure 25A** we can see the entire head of an L1 organism. A GFP MIP is shown to visualize the head in one plane. The interrupted projections in this head can be contrasted with the neat projections in **Figure 24.** Below the head are three panels of the CEPs in this animal. The panels are in descending order of health/viability. In **Figure 25B** we can see a relatively healthy CEPD- though already exhibiting signs of perinuclear clustering. There are many lysosomes and they are small. The cell is not swollen and its projection is intact. In **Figure 25C** a CEPV in the process of dying is seen. The cell is rounded and its projection has begun to

clear. The lysosomes seem to be fewer than in the healthier CEPD. We can see what appears to be enlarged lysosomes in the path of the dying projection. There is clear perinuclear clustering when the merged panel is considered. Finally, in **Figure 25D,** we can see a cell that is fading away. It is grossly enlarged in comparison to the other CEPs. Its projection is dotted and completely separated from the cell. The lysosome in this figure is enlarged and is singular. This may mean that a fusion of lysosomes has occurred, and one large lysosome in the end has been formed as a result. It also has migrated to the periphery of the nucleus. One CEPV has already died and been cleared- or if not entirely cleared then the LMP-1 proteins have been cleared.

These are initial observations and have yet to be quantified. Yet, they give us insight into the nature of cell death in the *trp-4(d)* model. In the mec-4(d) model, the lysosomes exhibit signs of perinuclear clustering and rupture (Artal-Sanz et al., 2006). Here, we can certainly see perinuclear clustering, however, lysosomal rupture has not been observed. The kinetics of the death cannot be ignored- this is a swift process. Thus, many more images or a time lapse will need to be generated in order to clarify the death events in this model.

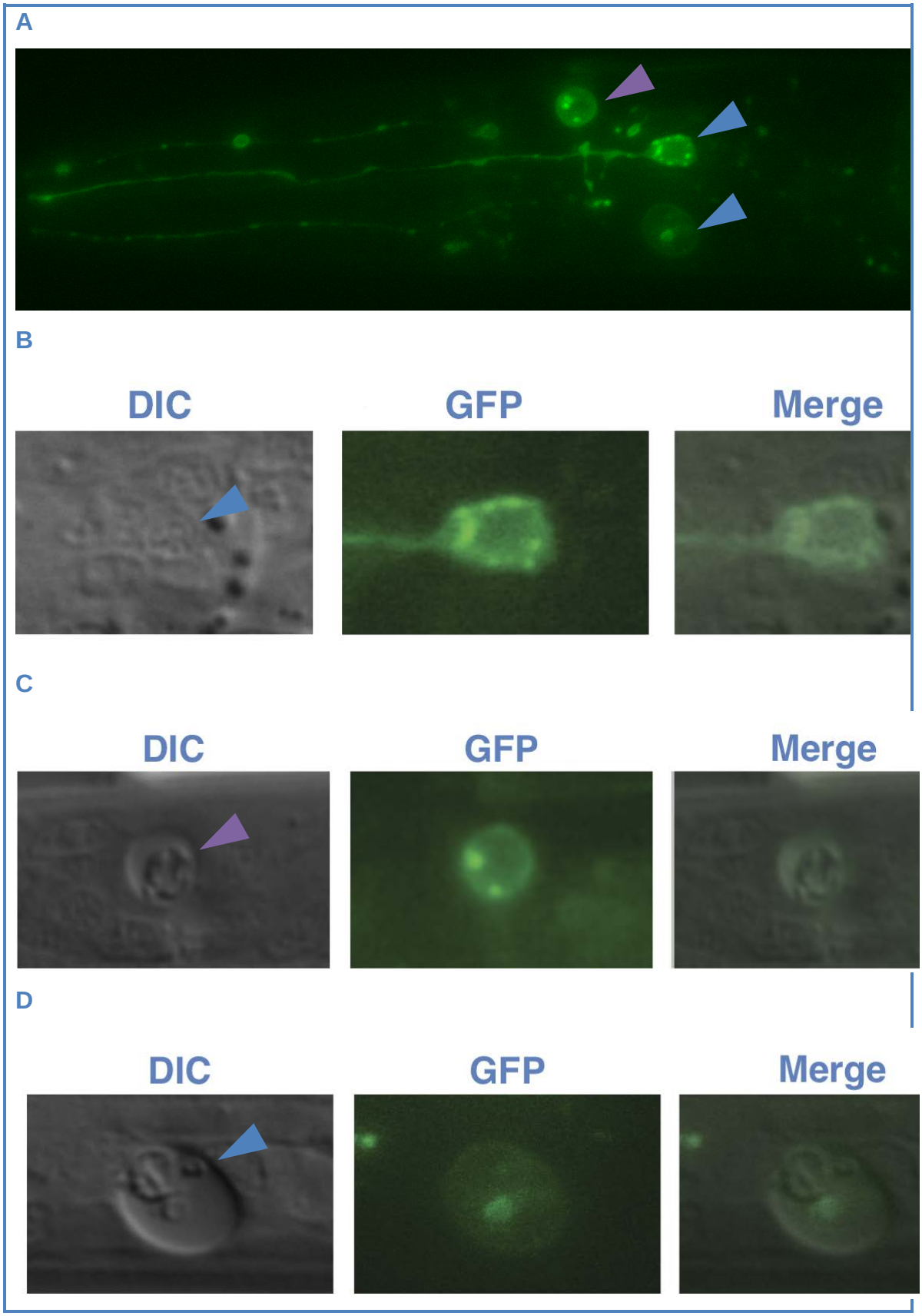
A
B
DIC
GFP
Merge
C
DIC
GFP
Merge
D
DIC
GFP
Merge

Figure 25 LMP-1::GFP in a *trp-4(d)* mutant is shown here. A shows the MIP of the GFP in the head. **B** shows a CEPD (blue uppermost arrow in **A**), **C** shows a CEPV (purple arrow), and **D** shows a CEPD (blue lower arrow in **A**). All images were taken at 100x of L1 organisms.

Additionally, crosses with suppressors of *trp-4(d)* degeneration can be completed, and further observations into the consequences of these suppressors to lysosomal morphology can be made. All of these morphological observations will provide insight into the subcellular events of *trp-4(d)* cell death.

In summary, the lysosomal acidification through V-ATPase pump, HS preconditioning, and lysosomal biogenesis were tested as candidate pathways for their involvement in *trp-4(d)* degeneration. All three of these candidates had successfully conferred protective effects in other models of neurodegeneration. Out of these three, lysosomal biogenesis has been uncovered as a potentially protective pathway in the *trp-4(d)* model and tools were generated for visualization of the lysosome in dopaminergic neurons. Protective trends in the other two explored pathways were also observed, which need further investigation.

HS preconditioning

It was previously reported that Heat Shock (HS) preconditioning protects the mechanosensory neurons from necrotic degeneration (Kourtis et al., 2012). To test whether such a protective effect can be seen for dopaminergic neurons in *trp-4(d)* mutant HS preconditioning will be referred to as simply HS, though this should not be confused with a true HS treatment, which is conducted at 39º as outlined by Kourtis et al.

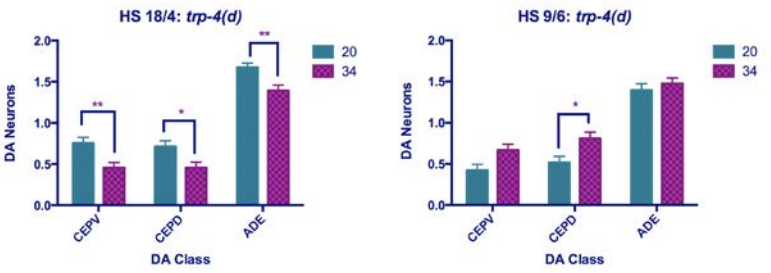

Figure 26 Effect of HS preconditioning on *trp-4(d)* neurodegeneration was completed two times, once on 18/4/2014 (left) and once on 9/6/2014 (right). For 18/4: At 20°, n=49; At 34°, n=46. For 9/6: At 20°, n=33, At 34°, n=42

Two separate experimental strategies were followed for exposure to heat, which are reflected in the

two scoring events in **Figure 26**. The first, strictly followed the protocol described in (Kourtis et al., 2012). In the second, the worms were left to nutate for one hour after the HS treatment to avoid developmental defects caused by the application of moderate heat at early embryonic stages. The two different methods resulted in two different trends, with a toxic effect seen in the first case, when the heat was applied too early, and a protective trend seen in the second. For all scorings, L1 animals were observed.

The experiment, following the first method, was also performed on *mec-4(d)* mutants as a positive control. In published results, there is a 66.7% decrease in cell corpses between the 20º and 34º treatments. While seeing a clear protective effect, not enough data were generated to be able to reliable use the *mec-4d* model as a positive control of our experimental conditions. The developmental and degeneration dynamics in the *mec-4(d)* model differ from the *trp-4(d);* familiarity with the mec-4(d) model could allow a proper comparison between the two models.

The first *trp-4(d)* scoring was completed with more individuals (At 20°, n=49; At 34°, n=46), thus the statistics that are performed on this data set provide more reliability than the other scoring event (At 20°, n=33: At 34°, n=42). Since there exist such variance between the two events, it is best to perform another round of experimentation with more individuals (n~100 for both temperatures) than to reflect deeply on either of these data sets.

Unbiased Approach

In addition to the more classical candidate approach, an unbiased approach was employed to discover novel mutations affecting *trp-4(d)* cell death. A screen for suppression of degeneration was chosen as the discovery method, and EMS was utilized as the mutagen. During four rounds of automated screening, three full suppressors and three partial suppressors were discovered in a screen, **Table 5**. The screening strain, *norSci1_[dat1::Trp-4(d)_unc-119]II; unc-119(ed3)III; trp-*

Table 5 Mutants isolated during the thesis are listed in this table. Historic, classification names are indicated at the end of the genotype. The screening strain for all of these was: *norSci1_[dat1::Trp-4(d)_unc-119]II; unc-119(ed3)III; trp-4(ot337)I;vtIs1*. Until WGS results are retuned, their molecular identity will remain unknown.

Strain	Genotype	Phenotype
MDH236	nor4;norSci1_[dat1::*Trp-4(d)*_unc-119]**II**;unc-119(ed3)**III**; trp-4(ot337)**I**;vtIs1**V**(2.6.2.3)	Full suppressor
MDH237	nor5;norSci1_[dat1::*Trp-4(d)*_unc-119]**II**;unc-119(ed3)**III**;trp-4(ot337)**I**;vtIs1**V**(2.12.3.1)	Full suppressor
MDH238	nor6;norSci1_[dat1::*Trp-4(d)*_unc-119]**II**;unc-119(ed3)**III**;trp-4(ot337)**I**;vtIs1**V**(2.7)	Full suppressor
MDH239	nor7;norSci1_[dat1::*Trp-4(d)*_unc-119]**II**;unc-119(ed3)**III**;trp-4(ot337)**I**;vtIs1**V**(1.5.6)	Partial suppressor in CEPs
MDH263	nor11;norSci1_[dat1::*Trp-4(d)*_unc-119]**II**;unc-119(ed3)**III**;trp-4(ot337)**I**;vtIs1**V**(3c41)	Partial suppressor in DA classes
MDH264	nor12;norSci1_[dat1::*Trp-4(d)*_unc-119]**II**;unc-119(ed3)**III**;trp-4(ot337)**I**;vtIs1**V**(35b)	Partial suppressor in ADEs

4(ot337)I;vtIs1[28], was developed after previous screens had failed to yield suppressors with intergenic mutations- mutations that did not occur on the *trp-4* locus itself. This strain has two copies of the mutated *trp-4(d)* gene: one endogenous copy and one Mosci single-copy insertion. The strategy behind using this strain was to reduce the probability of intragenic mutations. Though they would still happen, it is more probable that they would occur on one of the copies, but not both. This remained a possibility, just a less probable one.

Suspected full suppressors were confirmed to be intergenic by crossing to a wild type strain. A red fluorescent reporter (*otIs356[rab-3::NLS::tagRFP]V*) in the wild type strain was employed to distinguish cross progeny. The F_1 generation was

observed for degeneration. If degeneration was observed, we concluded that the mutant was a non-intragenic, recessive full suppressor and if none was observed, cross-progeny individuals were singled. If their progeny did not exhibit degenera-

[28] This was built by Mosci insertion by a post-doc in the lab, Janete Chung.

tion, the mutation was deemed intragenic, if it did, it was declared a dominant non-intragenic suppressor.

All six retrieved suppressors, **Figure 27**, were confirmed to be intergenic by crossing to a wild type strain. (as described above an in Materials and Methods section) Additionally, it was determined using standard genetic crosses with reporters on known chromosomes that the causative mutation most likely rests on chromosome III. Notably, none of the genetic suppressors for *trp-4(d)* reported so far in this thesis and in Nagarajan *et al.* lie on chromosome III.

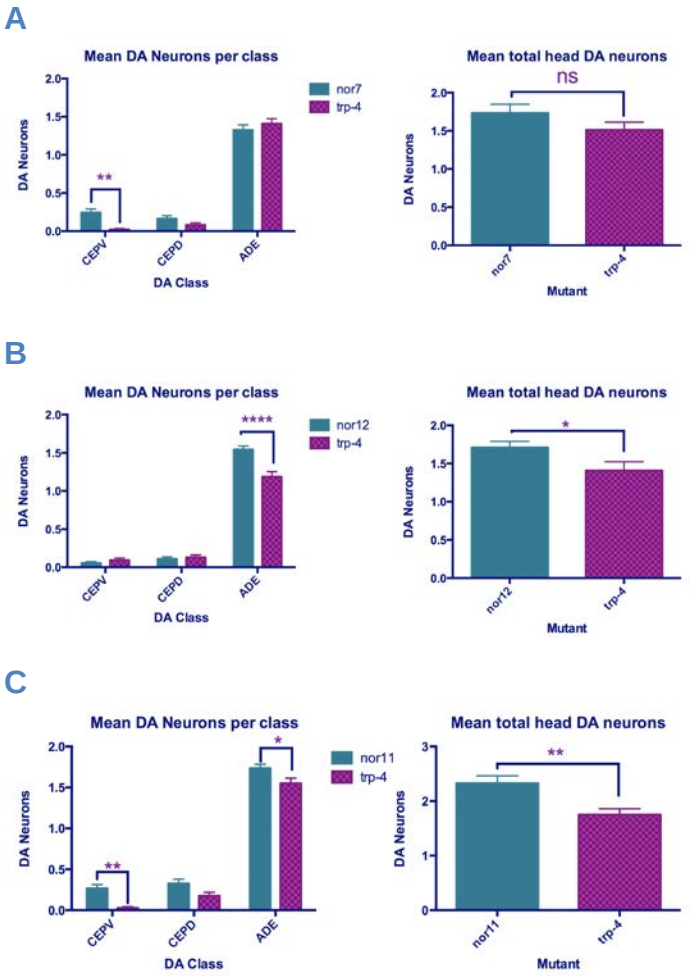

Figure 27 Partial Suppressors from EMS screens were (with their historic names): **A:** 1.5.6, **B:** 35B, and **C:** 3C41. Two-tailed unpaired t-test with Welch's correction determined significant for the Total DA Neurons graphs.

The full suppressors were sent out for whole genome sequencing. Upon the submission of this thesis, sequencing results are yet unavailable. When results are obtained, those mutations on chromosome III will be reviewed and tested. Analysis and characterization will be continued with the identification of the causative mutations in the full suppressors.

Conclusions & Future Directions

This thesis explored three pathways previously implicated in necrotic cell death in mechanosensory neurons, for their involvement in the degeneration of dopamine neurons in the *trp-4(d)* model. It also detailed the building of a new reporter, which will add morphological insight into trp-4(d) cell death. Finally, six suppressor mutants were isolated that will contribute to a novel understanding of *trp-4(d)* cell death.

Lysosomal acidification through V-ATPase Pump

The results gathered in this thesis, are not conclusive as to whether or not the V-ATPase pump plays a role in *trp-4(d)* degeneration. A protective trend when knocking down some subunits was observed (VHA-12, 3, 11 and 17), however more experiments are required. In order to determine if cellular acidification is a factor in *trp-4(d)* induced degeneration, it would be very useful to track the neuronal pH with pH sensitive reporters. Moreover, although knocking down single subunits of the V-ATPase pump has not yielded thus far strong suppression, by building double mutants with *vha* genes more than mild protection may be seen. If the *vha-12* and *vha-3* mutations are proven protective through more scorings, it would be interesting to know whether this effect is because of its role in lysosomal acidification or via a different mechanism.

Further pursuing the pharmacological approach can give a more determinate answer as to the involvement of the pump. For this, the Bafilomycin protocol needs to be optimized in order to determine the most effective means of treatment for the heavily-protected embryos.

Lysosomal Biogenesis

Interference with GLO-1 function has resulted in a suppression in *trp-4(d)* cell death. This result points to an involvement of the lysosomal biogenesis path-

ways in our cell death model. Expression of *glo-1* has been reported to only be in the intestine. However, this is not certain, as in the publication images (Hermann et al., 2005) only the intestine is visible in the adult DIC image. Moreover, it is possible that its expression is highest in the gut and minimal enough in DA neurons to have gone unnoticed- a phenotype can only be known once it is looked for. The question remains as to whether or not *glo-1* is expressed in dopaminergic neurons in C. elegans. If it is not, than either this result is an artefact of the strain we used or the suppression is the result of a cell- non-autonomous pathway. In order to address the former question another allele of *glo-1* should be scored in *trp-4(d)* mutants. To address the latter question, cell specific rescue can be performed, by expressing *glo-1* specifically in the dopaminergic neurons and complementary cell specific rescue in other tissues.

Additionally, the *glo-1* mutant should be crossed with the LMP-1::GFP reporter to determine if the lysosomal morphology is affected in *trp-4(d)* mutants and how it is different, if at all, in *glo-1;trp-4* mutants. *glo-1* was discovered as defective in gut granule biogenesis. Should the DA neurons indeed contain similar LRO, this would also implicate DA neurons in *C. elegans* to be a melanosome like cell-containing a pigment molecule (Coburn and Gems, 2013) (Raposo and Marks, 2007). The birefringent matter in the gut granules is a kynurenine pathway product and kynurenine pathway dysregulation has been implicated in many neurodegenerative diseases as well as acute insults (Vecsei et al., 2013) (Stone et al., 2012).

cup-5 mutants should also be crossed with *trp-4(d)* mutants to explore whether they will have the opposite effect to the *glo-1* mutants. While *glo-1* mutants impair lysosomal biogenesis, *cup-5* mutants promote the formation of lysosomes and thus exacerbate necrosis in the *mec-4(d)* model (Artal-Sanz et al., 2006).

HS Preconditioning

Further experiments are required to determine whether induction of stress responses, like the heat shock response induced after preconditioning, is protective

to neuronal cell death in the *trp-4(d)* model. The HS preconditioning method needs to be improved, and potentially other stress response pathways can be explored.

Forward Genetic Screen

Undertaking an unbiased approach, three partial and three full suppressors of *trp-4(d)* cell death were discovered in the course of this thesis. The partial suppressors come from two rounds of screening and the full suppressors come from one round. Given the rarity of any suppression experienced in previously conducted screens, three unique full suppressors would be extraordinary based on the P_0 population (Less than the recommended in **Figure 15A**). It is most likely that these are siblings. However, even one true full suppressor will provide great insight into the mechanism of *trp-4(d)* mediated neurodegeneration. Moreover, the three partial suppressors could also potential uncover novel players in this pathway.

The TRP-4d Model

The TRP-4d model of cell death could potentially be an important one in studies of neurodegeneration. It shares many features with existing models, such as its necrotic presentation and its resemblance to excitotoxic death. Yet, it is distinct in others, like its progressive manifestation. The implication of the lysosome in its mechanisms additionally makes it an attractive model for neurodegenerative studies- as this is a topic undergoing much research. The fact that TRP-4d degeneration affects dopaminergic neurons opens two perspectives. The first of which is that this model can be used to identify DA-specific ways to suppress degeneration. Furthermore, it would be interesting whether polymorphisms in human TRP channels are associated with PD.

In order to implicate the TRP-4d model as an important in cell death pathways, more characterization is necessary. Events in cell death pathways are not random, as demonstrated by many models. The use of microfluidics, nano-beads, or

other means of constant monitoring of one worm over a period of time is necessary to describe the intracellular degeneration dynamics in order to further establish the *trp-4* model and its use in neurodegeneration studies.

It would be useful to determine the basal slowing response in L1 organisms. As this is when the degeneration is proposed to begin. In addition, lifespan of *trp-4* mutants is not established and should be to provide a baseline for aging studies.

Assuming that TRP-4d is a very “aggressive” channel, one could cross the suppressed degeneration mutant *crt-1;trp-4* with any of the most promising of the candidates tested here. Thus, any mild suppression that would have been ruled insignificant otherwise, could manifest, and possibly yield a synergistic effect.

Localization of the trp-4 channel should also be determined. It was previously shown to be located on the cell membrane; Is it also located on the membrane of an organelle, or possibly many organelles? Does such localization contribute to the observed neuronal damage?

As with most research projects, this thesis began with a set of questions and has ended with new questions. The lysosome has been implicated in *trp-4(d)* degeneration, and this relationship should be further probed and explored.

References

Ahringer, J. (2006) 'Reverse genetics', in Ambros, V. (ed.) *WormBook*.

Altun, Z. F. a. H., D.H. (2009) 'Pericellular structures', *WormAtlas*.

Artal-Sanz, M., Samara, C., Syntichaki, P. and Tavernarakis, N. (2006) 'Lysosomal biogenesis and function is critical for necrotic cell death in Caenorhabditis elegans', *J Cell Biol,* 173(2), pp. 231-9.

Bianchi, L., Gerstbrein, B., Frokjaer-Jensen, C., Royal, D. C., Mukherjee, G., Royal, M. A., Xue, J., Schafer, W. R. and Driscoll, M. (2004) 'The neurotoxic MEC-4(d) DEG/ENaC sodium channel conducts calcium: implications for necrosis initiation', *Nat Neurosci,* 7(12), pp. 1337-44.

Bjorklund, A. and Dunnett, S. B. (2007) 'Dopamine neuron systems in the brain: an update', *Trends Neurosci,* 30(5), pp. 194-202.

Black, R. A., Kronheim, S. R., Cantrell, M., Deeley, M. C., March, C. J., Prickett, K. S., Wignall, J., Conlon, P. J., Cosman, D., Hopp, T. P. and et al. (1988) 'Generation of biologically active interleukin-1 beta by proteolytic cleavage of the inactive precursor', *J Biol Chem,* 263(19), pp. 9437-42.

Brenner, S. (1974) 'The genetics of Caenorhabditis elegans', *Genetics,* 77(1), pp. 71-94.

Brenner, S. (2003) 'Nobel lecture. Nature's gift to science', *Biosci Rep,* 23(5-6), pp. 225-37.

Calabrese, E. J. (2004) 'Hormesis: a revolution in toxicology, risk assessment and medicine', *EMBO Rep,* 5 Spec No, pp. S37-40.

Chu, Y., Morfini, G. A., Langhamer, L. B., He, Y., Brady, S. T. and Kordower, J. H. (2012) 'Alterations in axonal transport motor proteins in sporadic and experimental Parkinson's disease', *Brain,* 135(Pt 7), pp. 2058-73.

Clark, I. E., Dodson, M. W., Jiang, C., Cao, J. H., Huh, J. R., Seol, J. H., Yoo, S. J., Hay, B. A. and Guo, M. (2006) 'Drosophila pink1 is required for mitochondrial function and interacts genetically with parkin', *Nature,* 441(7097), pp. 1162-6.

Coburn, C. and Gems, D. (2013) 'The mysterious case of the C. elegans gut granule: death fluorescence, anthranilic acid and the kynurenine pathway', *Front Genet,* 4, pp. 151.

Conforti, L., Adalbert, R. and Coleman, M. P. (2007) 'Neuronal death: where does the end begin?', *Trends Neurosci,* 30(4), pp. 159-66.

Dehay, B., Martinez-Vicente, M., Caldwell, G. A., Caldwell, K. A., Yue, Z., Cookson, M. R., Klein, C., Vila, M. and Bezard, E. (2013) 'Lysosomal impairment in Parkinson's disease', *Mov Disord,* 28(6), pp. 725-32.

Dexter, P. M., Caldwell, K. A. and Caldwell, G. A. (2012) 'A predictable worm: application of Caenorhabditis elegans for mechanistic investigation of movement disorders', *Neurotherapeutics,* 9(2), pp. 393-404.

Doitsidou, M., Flames, N., Lee, A. C., Boyanov, A. and Hobert, O. (2008) 'Automated screening for mutants affecting dopaminergic-neuron specification in C. elegans', *Nat Methods,* 5(10), pp. 869-72.

Doitsidou, M., Flames, N., Topalidou, I., Abe, N., Felton, T., Remesal, L., Popovitchenko, T., Mann, R., Chalfie, M. and Hobert, O. (2013) 'A combinatorial regulatory signature controls terminal differentiation of the dopaminergic nervous system in C. elegans', *Genes Dev,* 27(12), pp. 1391-405.

Driscoll, M. and Chalfie, M. (1991) 'The mec-4 gene is a member of a family of Caenorhabditis elegans genes that can mutate to induce neuronal degeneration', *Nature,* 349(6310), pp. 588-93.

Elmore, S. (2007) 'Apoptosis: a review of programmed cell death', *Toxicol Pathol,* 35(4), pp. 495-516.

Ernstrom, G. G., Weimer, R., Pawar, D. R., Watanabe, S., Hobson, R. J., Greenstein, D. and Jorgensen, E. M. (2012) 'V-ATPase V1 sector is required for corpse clearance and neurotransmission in Caenorhabditis elegans', *Genetics,* 191(2), pp. 461-75.

Fedorow, H., Tribl, F., Halliday, G., Gerlach, M., Riederer, P. and Double, K. L. (2005) 'Neuromelanin in human dopamine neurons: comparison with peripheral melanins and relevance to Parkinson's disease', *Prog Neurobiol,* 75(2), pp. 109-24.

Fink, S. L. and Cookson, B. T. (2005) 'Apoptosis, pyroptosis, and necrosis: mechanistic description of dead and dying eukaryotic cells', *Infect Immun,* 73(4), pp. 1907-16.

Galluzzi, L., Vitale, I., Abrams, J. M., Alnemri, E. S., Baehrecke, E. H., Blagosklonny, M. V., Dawson, T. M., Dawson, V. L., El-Deiry, W. S., Fulda, S., Gottlieb, E., Green, D. R., Hengartner, M. O., Kepp, O., Knight, R. A., Kumar, S., Lipton, S. A., Lu, X., Madeo, F., Malorni, W., Mehlen, P., Nunez, G., Peter, M. E., Piacentini, M., Rubinsztein, D. C., Shi, Y., Simon, H. U., Vandenabeele, P., White, E., Yuan, J., Zhivotovsky, B., Melino, G. and Kroemer, G. (2012) 'Molecular definitions of cell death subroutines: recommendations of the Nomenclature Committee on Cell Death 2012', *Cell Death Differ,* 19(1), pp. 107-20.

Gees, M., Owsianik, G., Nilius, B. and Voets, T. (2012) 'TRP channels', *Compr Physiol,* 2(1), pp. 563-608.

Golstein, P. and Kroemer, G. (2007) 'Cell death by necrosis: towards a molecular definition', *Trends Biochem Sci,* 32(1), pp. 37-43.

Bachelor's Thesis, Håland, M. (2014) *Identification of genetic modifiers of dopaminergic neuronal degeneration in C. elegans with special focus on autophagy* Bachelor, University of Stavanger, Stavanger, NO.

Herman, R. K. (2005) 'Introduction to sex determination', in Community, T.C.e.R. (ed.) *WorkBook*.

Hermann, G. J., Schroeder, L. K., Hieb, C. A., Kershner, A. M., Rabbitts, B. M., Fonarev, P., Grant, B. D. and Priess, J. R. (2005) 'Genetic analysis of lysosomal trafficking in Caenorhabditis elegans', *Mol Biol Cell,* 16(7), pp. 3273-88.

Hodgkin, J., Horvitz, H. R. and Brenner, S. (1979) 'Nondisjunction Mutants of the Nematode CAENORHABDITIS ELEGANS', *Genetics,* 91(1), pp. 67-94.

Hong, K. and Driscoll, M. (1994) 'A transmembrane domain of the putative channel subunit MEC-4 influences mechanotransduction and neurodegeneration in C. elegans', *Nature,* 367(6462), pp. 470-3.
Jorgensen, E. M. and Mango, S. E. (2002) 'The art and design of genetic screens: caenorhabditis elegans', *Nat Rev Genet,* 3(5), pp. 356-69.
Kang, L., Gao, J., Schafer, W. R., Xie, Z. and Xu, X. Z. (2010) 'C. elegans TRP family protein TRP-4 is a pore-forming subunit of a native mechanotransduction channel', *Neuron,* 67(3), pp. 381-91.
Kerr, J. F., Wyllie, A. H. and Currie, A. R. (1972) 'Apoptosis: a basic biological phenomenon with wide-ranging implications in tissue kinetics', *Br J Cancer,* 26(4), pp. 239-57.
Klionsky, D. J. (2007) 'Autophagy: from phenomenology to molecular understanding in less than a decade', *Nat Rev Mol Cell Biol,* 8(11), pp. 931-7.
Kostich, M., Fire, A. and Fambrough, D. M. (2000) 'Identification and molecular-genetic characterization of a LAMP/CD68-like protein from Caenorhabditis elegans', *J Cell Sci,* 113 (Pt 14), pp. 2595-606.
Kourtis, N., Nikoletopoulou, V. and Tavernarakis, N. (2012) 'Small heat-shock proteins protect from heat-stroke-associated neurodegeneration', *Nature,* 490(7419), pp. 213-8.
Kroemer, G., Galluzzi, L., Vandenabeele, P., Abrams, J., Alnemri, E. S., Baehrecke, E. H., Blagosklonny, M. V., El-Deiry, W. S., Golstein, P., Green, D. R., Hengartner, M., Knight, R. A., Kumar, S., Lipton, S. A., Malorni, W., Nunez, G., Peter, M. E., Tschopp, J., Yuan, J., Piacentini, M., Zhivotovsky, B., Melino, G. and Nomenclature Committee on Cell, D. (2009) 'Classification of cell death: recommendations of the Nomenclature Committee on Cell Death 2009', *Cell Death Differ,* 16(1), pp. 3-11.
Kroemer, G. and Levine, B. (2008) 'Autophagic cell death: the story of a misnomer', *Nat Rev Mol Cell Biol,* 9(12), pp. 1004-10.
Lakso, M., Vartiainen, S., Moilanen, A. M., Sirvio, J., Thomas, J. H., Nass, R., Blakely, R. D. and Wong, G. (2003) 'Dopaminergic neuronal loss and motor deficits in Caenorhabditis elegans overexpressing human alpha-synuclein', *J Neurochem,* 86(1), pp. 165-72.
Li, W., Feng, Z., Sternberg, P. W. and Xu, X. Z. (2006) 'A C. elegans stretch receptor neuron revealed by a mechanosensitive TRP channel homologue', *Nature,* 440(7084), pp. 684-7.
Lockshin, R. A. and Williams, C. M. (1965) 'Programmed Cell Death--I. Cytology of Degeneration in the Intersegmental Muscles of the Pernyi Silkmoth', *J Insect Physiol,* 11, pp. 123-33.
Lockshin, R. A. and Zakeri, Z. (2001) 'Programmed cell death and apoptosis: origins of the theory', *Nat Rev Mol Cell Biol,* 2(7), pp. 545-50.
Bachelor's Thesis, Maugard, M. (2013) *Genetic factors involved in dopaminergic neurons degeneration under trp-4 mutation.* Bachelor, UPMC and Ecole Normale Sup´ erieure, Universitetet i Stavanger.
Mazzulli, J. R., Xu, Y. H., Sun, Y., Knight, A. L., McLean, P. J., Caldwell, G. A., Sidransky, E., Grabowski, G. A. and Krainc, D. (2011) 'Gaucher disease

glucocerebrosidase and alpha-synuclein form a bidirectional pathogenic loop in synucleinopathies', *Cell,* 146(1), pp. 37-52.
Mehta, A., Prabhakar, M., Kumar, P., Deshmukh, R. and Sharma, P. L. (2013) 'Excitotoxicity: bridge to various triggers in neurodegenerative disorders', *Eur J Pharmacol,* 698(1-3), pp. 6-18.
Nagarajan, A., Ning, Y., Reisner, K., Buraei, Z., Larsen, J. P., Hobert, O. and Doitsidou, M. (2014) 'Progressive degeneration of dopaminergic neurons through TRP channel-induced cell death', *J Neurosci,* 34(17), pp. 5738-46.
Neff, M. M., Turk, E. and Kalishman, M. (2002) 'Web-based primer design for single nucleotide polymorphism analysis', *Trends Genet,* 18(12), pp. 613-5.
Nicotera, P. and Melino, G. (2004) 'Regulation of the apoptosis-necrosis switch', *Oncogene,* 23(16), pp. 2757-65.
Park, J., Lee, S. B., Lee, S., Kim, Y., Song, S., Kim, S., Bae, E., Kim, J., Shong, M., Kim, J. M. and Chung, J. (2006) 'Mitochondrial dysfunction in Drosophila PINK1 mutants is complemented by parkin', *Nature,* 441(7097), pp. 1157-61.
Parkinson, J. (1817) *An essay on the shaking palsy.* London: Printed by Whittingham and Rowland for Sherwood.
Pujol, N., Bonnerot, C., Ewbank, J. J., Kohara, Y. and Thierry-Mieg, D. (2001) 'The Caenorhabditis elegans unc-32 gene encodes alternative forms of a vacuolar ATPase a subunit', *J Biol Chem,* 276(15), pp. 11913-21.
Raff, M. C. (1992) 'Social controls on cell survival and cell death', *Nature,* 356(6368), pp. 397-400.
Raposo, G. and Marks, M. S. (2007) 'Melanosomes--dark organelles enlighten endosomal membrane transport', *Nat Rev Mol Cell Biol,* 8(10), pp. 786-97.
Sieburth, D., Ch'ng, Q., Dybbs, M., Tavazoie, M., Kennedy, S., Wang, D., Dupuy, D., Rual, J. F., Hill, D. E., Vidal, M., Ruvkun, G. and Kaplan, J. M. (2005) 'Systematic analysis of genes required for synapse structure and function', *Nature,* 436(7050), pp. 510-7.
Singson, A., Hill, K. L. and L'Hernault, S. W. (1999) 'Sperm competition in the absence of fertilization in Caenorhabditis elegans', *Genetics,* 152(1), pp. 201-8.
Stiernagle, T. (2006) ' Maintenance of C. elegans', in Fay, D. (ed.) *WormBook: The Online Review of C. elegans Biology [Internet]*. Minnespta, MN: CGC.
Bachelor's Thesis, Strenitz, M. (2014) *Genetic enhancers and suppressors of dopaminergic cell death in C. elegans with special focus on apoptosis.* Bachelor, University of Stavanger, Stavanger, NO.
Sulston, J. E. and Horvitz, H. R. (1977) 'Post-embryonic cell lineages of the nematode, Caenorhabditis elegans', *Dev Biol,* 56(1), pp. 110-56.
Syntichaki, P., Samara, C. and Tavernarakis, N. (2005) 'The vacuolar H+ -ATPase mediates intracellular acidification required for neurodegeneration in C. elegans', *Curr Biol,* 15(13), pp. 1249-54.
Syntichaki, P. and Tavernarakis, N. (2003) 'The biochemistry of neuronal necrosis: rogue biology?', *Nat Rev Neurosci,* 4(8), pp. 672-84.

Syntichaki, P., Xu, K., Driscoll, M. and Tavernarakis, N. (2002) 'Specific aspartyl and calpain proteases are required for neurodegeneration in C. elegans', *Nature,* 419(6910), pp. 939-44.

Timmons, L., Court, D. L. and Fire, A. (2001) 'Ingestion of bacterially expressed dsRNAs can produce specific and potent genetic interference in Caenorhabditis elegans', *Gene,* 263(1-2), pp. 103-12.

Treusch, S., Knuth, S., Slaugenhaupt, S. A., Goldin, E., Grant, B. D. and Fares, H. (2004) 'Caenorhabditis elegans functional orthologue of human protein h-mucolipin-1 is required for lysosome biogenesis', *Proc Natl Acad Sci U S A,* 101(13), pp. 4483-8.

Tucci, M. L., Harrington, A. J., Caldwell, G. A. and Caldwell, K. A. (2011) 'Modeling dopamine neuron degeneration in Caenorhabditis elegans', *Methods Mol Biol,* 793, pp. 129-48.

Venkatachalam, K. and Montell, C. (2007) 'TRP channels', *Annu Rev Biochem,* 76, pp. 387-417.

Werle, E., Schneider, C., Renner, M., Volker, M. and Fiehn, W. (1994) 'Convenient single-step, one tube purification of PCR products for direct sequencing', *Nucleic Acids Res,* 22(20), pp. 4354-5.

Xu, K., Tavernarakis, N. and Driscoll, M. (2001) 'Necrotic cell death in C. elegans requires the function of calreticulin and regulators of Ca(2+) release from the endoplasmic reticulum', *Neuron,* 31(6), pp. 957-71.

Yang, Y., Gehrke, S., Imai, Y., Huang, Z., Ouyang, Y., Wang, J. W., Yang, L., Beal, M. F., Vogel, H. and Lu, B. (2006) 'Mitochondrial pathology and muscle and dopaminergic neuron degeneration caused by inactivation of Drosophila Pink1 is rescued by Parkin', *Proc Natl Acad Sci U S A,* 103(28), pp. 10793-8.

Ye, J., Coulouris, G., Zaretskaya, I., Cutcutache, I., Rozen, S. and Madden, T. L. (2012) 'Primer-BLAST: a tool to design target-specific primers for polymerase chain reaction', *BMC Bioinformatics,* 13, pp. 134.

Appendix

Crossing Schemes

1 General cross

Crossing unc-32(e189) into trp-4(ot337)

1. Cross 697♂ with 421♀

697. unc-32(e189)III; him-8(e1489)IV ♂ X 421. trp-4(ot337)I; vtIs1V♀

- e189 is a recessive mutation, the unc is a coiler

2. Pick 10 F1s

$$\frac{ot337}{+}(I);\frac{e189}{+}(III);\frac{him-8}{+}(IV);\frac{vtIs1}{+}(V)$$

3. Single 30 green coilers F2s

- ignoring him-8 from this point on

ot337	*e189*	*vtIs1*
$\frac{ot337}{ot337}(I)$	$\frac{e189}{e189}(III)$	$\frac{vtIs1}{vtIs1}(V)$
$\frac{ot337}{+}(I)$	$\frac{e189}{+}(III)$	$\frac{vtIs1}{+}(V)$
$\frac{+}{ot337+}(I)$	$\frac{+}{e189}(X)$	$\frac{+}{vtIs1}(V)$
$\frac{+}{+}(I)$	$\frac{+}{+}(X)$	$\frac{+}{+}(V)$

4. In next generation, find plates that are green and coiler homozygous.

See the status of degeneration at this point, are there clear distinctions between WT and non? If so, then also **keep plates that are not WT.**

5. Genotype for ot337 and e189

6. Keep plates that are homozygous for both and this should also be green homozygous.

2 Cross involving the X chromosome

Crossing vha-12(n2915sd) and trp-4;vtIs1

. Make males with N2

663.vha-12(n2915sd)(X)

$\frac{n2915sd}{0}(X)$

. Cross males into 421 hermaphrodites

$\frac{n2915sd}{0}(X)$**X** ot337(I); vtIs1(V)

*n2915sd will now be hemizygous, ensuring you will only get heterozygous hermaphrodites for n2915sd

. Pick 10 F1s

$$\frac{ot337}{+}(I);\frac{+}{vtIs1}(V);\frac{n2915sd}{+}(x)$$

. Confirm 'correct' F1 plates

*These will have mixed populations for degeneration and green

. Pick 30 green non-WT worms from correct plates

ot337	*n2915sd*	*vtIs1*
$\frac{ot337}{+}(I)$	$\frac{n2915sd}{n2915sd}(X)$	$\frac{+}{+}(V)$
$\frac{ot337}{+}(I)$	$\frac{n2915sd}{+}(X)$	$\frac{+}{vtIs1}(V)$
$\frac{ot337}{ot337}(I)$	$\frac{n2915sd}{+}(X)$	$\frac{vtIs1}{+}(V)$
$\frac{+}{+}(I)$	$\frac{+}{+}(X)$	$\frac{vtIs1}{vtIs1}(V)$

Genotype for n2915sd

Score head neurons for degeneration in the new strain against 421

Primers

Under the primer sequences is the predicated molecular characterization. After TP73, the oligo calculator on the IDT technologies website was used. Only primers used in this thesis are included, so there are gaps in the numbering.

#	F/R	GENE/Restriction^Site/nucleotides	Name/Use	Notes
TP35	F	TTGATCAGCTGGAACGAGAA	VHA-7, OK1952 external	NCBI: WT: 2747
		56.87	45.00	
TP36	R	GAACTGTAGCCGGTGGGAAT		
		59.75	55.00	
TP37	F	AAGTTCCAAGGATGAGGGCG	Vha-3, ok1501external	NCBI: Wt: 1359
		60.04	55.00	
TP38	R	AGTCGCAGGAAATGCTCGAA		
		60.04	50.00	
TP39	F	CAGACGCAGTAAGAAACGGC	Vha-12, ok821 external	NCBI
		59.56	55.00	
TP40	R	ACGTAGATCTGTCCCTCGGT		
		59.74	55.00	
TP41	F	CGTTCCGGACAGGTTCTTGA	VHA-12, OK821 INTERNAL	NCBI
		59.97	55.00	
TP42	R	CCAAGAAGTCCTCGGCAAGT		
		59.96	55.00	

TP43	F	TTTGTCGCCGGAGTTCTACC	Vha-7, ok1952 INTERNAL	Ncbi Wt: 271
		60.04	55.00	
TP44	R	AGCGGATTTTTCTCACCCGT		
		59.96	50.00	
TP45	F	TCGTGGCTATGGTTCTCAAGG	VHA-2, OK619 EXTERNAL	Ncbi: Wt: 1827
		59.79	52.38	
TP46	R	GCAGTGCAGGTGGTAAAAGC		
		60.04	55.00	
TP47	F	TCTTTCGGCGGTTTCCAAGT	VHA-3, OK1501 INTERNAL	Ncbi: Wt: 459
		60.18	50.00	
TP48	R	CGCAATAGTTCGTCACGGTC		
		59.36	55.00	
TP49	F	ACGACGACTTGTCTCCGTTT	VHA-2, OK619 INTERNAL	Ncbi: Wt: 372 Mut: 0
TP50	R	CATACCTGTTCTCCCGTGGC		
TP54	R	GAAACTCGATGGATATTTTTGCAAAAGCT		
TP57	F	TATTGACCACCTTGTTCAGTGGAGAGTAC	DCAPS, glo-1 zu391 (2 mis-mmatches) ATCACT->>AGT*ACT (ScaI)	
TP58	R	ACAAAGCGATGAAATCCCTCTCA		
TP59	F	tcatcggaatgacagacttgg	Glo-1 zu391 external primer	
TP60	F	taccgttttggcaacattccg	Lmp-1 externals	From Andrew fire paper (lmp-1 discovery)
TP61	R	ggcaaaccaaggtaattcaacaacc		

TP62	F	AGACTTGGTCAGTTGGGAAAACGGTGC	INTERNAL LMP-1	
TP63	R	gttttcgctacacgtaggctgaatgc Tm: 58	EXTERNAL LMP-1	
TP64	F	ttggagGGTACCATGTTGAAATCGTTTGTCATCTTG Tm: 60	FOR CLONING- introduces KPNI at N-terminus of lmp-1	
TP65	R	gttgGAATTCCTATTTGTATAGTTCATCCATGC Tm: 58	For cloning- introduces ECORI site at COOH of GFP	
TP66	F	tcagGGATCCATGTTGAAATCGTTTGTCATCTTG 62	Cloning strategy 2- introduces BAMHI at NH3 of lmp-1	
TP67	R	CTACCGGTACCAA**G**ACGCTGGCATATCCTTGTC 62	Cloning strategy 2-introduces KPNI at COOH of lmp-1	
TP68				
TP69	F	GCTTGTTGTCTTGACCGACA	Primers for vha-12	
TP70	R	CTAGTACCTTGGGTGATGAAG		
TP71	F	GAGACGGATCAATCACACAAA	Reverse primer is DCAPS These will genotype vha-12 (n2915sd)	
TP72	**R**	GATCTTCTCTTGTCATTCCTTCTCTTATA		
TP76	F	AGA TGT CCA GGC GAT GAA GG LENGTH: 20 GC CONTENT: 55.0 % MELT TEMP: 64.7 °C		
TP77	F	GTC TTG TTC GTA TCC TTC TCC LENGTH: 21 GC CONTENT: 47.6 % MELT TEMP: 61.0 °C	UNC-32 (E189) SNP Reverse primer is DCAPS Cuts mutant with	DCAPS program, me
TP78	R	GGTGGCAACATTTCTCCAGTCCCAGC		

			AluI	
TP79	R	atacaacgacgagtaggagc LENGTH: 20 GC CONTENT: 50.0 % MELT TEMP: 62.1 °C	For e189, after DCAPS, can be used with TP77 for sequencing	Product: 356
TP 80	F	ATCCTGTGACAGTTCTCTCG LENGTH: 20 GC CONTENT: 50.0 % MELT TEMP: 62.3 °C	For apb-3(ok492)	External MUT:411 WT:1477
TP81	R	GCATCCATTATTTGACGACTT LENGTH: 21 GC CONTENT: 38.1 % MELT TEMP: 60.9 °C		
TP82	R	CGTTCCTTGAAACTACTAATAA LENGTH: 22 GC CONTENT: 31.8 % MELT TEMP: 58.3 °C	For apb-3(ok492)	Internal Mut:0 Wt:562
TP83	F	AAGAAGAGGATGATAGTGAGC LENGTH: 21 GC CONTENT: 42.9 % MELT TEMP: 60.6 °C		
TP84	F	TTTGAACGCCTCCTCAATGC LENGTH: 20 GC CONTENT: 50.0 % MELT TEMP: 64.6 °C	For glo-1 (zu439) This mutation changes trp-106 into a stop codon	
TP85	R	ACACATTGATCACAGTGTGC LENGTH: 20 GC CONTENT: 45.0 % MELT TEMP: 62.5 °C		